KAUNAS UNIVERSITY OF TECHNOLOGY
FACULTY OF MECHANICAL ENGINEERING AND DESIGN

Vinod Raj Begur Venkataraj

DESIGN AND ANALYSIS OF WANKEL ENGINE

Master's Degree Final Project

Supervisor
Assoc. prof. dr. Sigitas Kilikevičius

KAUNAS, 2017

KAUNAS UNIVERSITY OF TECHNOLOGY
FACULTY OF MECHANICAL ENGINEERING AND DESIGN

DESIGN AND ANALYSIS OF WANKEL ENGINE

Master's Degree Final Project
Mechanical Engineering (code 621H30001)

Supervisor
(signature)Assoc. prof. dr. Sigitas Kilikevičius
(date)

Reviewer
(signature) Assoc. prof. dr. Povilas Krasauskas
(date)

Project made by
(signature) Vinod Raj Begur Venkataraj
(date)

KAUNAS, 2017

KAUNAS UNIVERSITY OF TECHNOLOGY

Faculty of Mechanical Engineering and Design
(Faculty)

Vinod Raj Begur Venkataraj
(Student's name, surname)

Mechanical Engineering, 621H30001
(Title and code of study programme)

DESIGN AND ANALYSIS OF WANKEL ENGINE

DECLARATION OF ACADEMIC HONESTY

2017 June 14
Kaunas

I confirm that a final project by me, **Vinod Raj Begur Venkataraj**, on the subject "Design and Analysis of Wankel Engine" is written completely by myself; all provided data and research results are correct and obtained honestly. None of the parts of this thesis have been plagiarized from any printed or Internet sources, all direct and indirect quotations from other resources are indicated in literature references. No monetary amounts not provided for by law have been paid to anyone for this thesis.

I understand that in case of a resurfaced fact of dishonesty penalties will be applied to me according to the procedure effective at Kaunas University of Technology.

(name and surname filled in by hand) *(signature)*

ACKNOWLEDGEMENT

I would like to express my sincere gratitude to Assoc. prof. dr. Sigitas Kilikevičius for his valuable inputs and supervising me throughout my research thesis.

Vinod Raj Begur Venkataraj

KAUNAS UN IVERSITY OF TECHNOLOGY
FACULTY OF MECHANICAL ENGINEERING AND DESIGN

Approved:
Head of Mechanical Engineering Department

(Signature, date)

Vytautas Grigas
(Name, Surname)

Head of Study Programmes in the Field of Mechanical Engineering

(Signature, date)

Kęstutis Pilkauskas
(Name, Surname)

MASTER STUDIES FINAL PROJECT TASK ASSIGNMENT
Study programme MECHANICAL ENGINERING - 621H30001

Approved by the Dean's Order No. V25-11-7 of May 3rd, 2017 y

Assigned to the student Vinod Raj Begur Venkataraj
(Name, Surname)

1. Title of the Project

Design and Analysis of Wankel Engine

2. Aim of the project

The aim of the thesis is to design internal combustion Wankel engine with an improved new apex seal.

3. Tasks of the project

Summary, Introduction, Literature review (selection of engine type, CFD analysis, methodology of calculation of fatigue life and K-factor influence), An illustration on the (3D model created, Kinematic study), CFD simulation for whole designed Wankel engine, Static FEA study is conducted to rotor (fatigue analysis for rotor and numerical calculation of rotor life), K-factor influence (designed different rotary profile, CFD for different K-factor), 3D assembly and Drafting.

4. Specific Requirements

- The engine is designed with improved new apex seal and with all calculation.
- The K-factor should be considered before designing rotary profile.

5. This task assignment is an integral part of the final project

6. Project submission deadline: 2017 May 19th.

Task Assignment received Vinod Raj Begur Venkataraj _____
(*Name, Surname of the Student*) (*Signature, date*)

Supervisor Assoc. prof. Dr Sigitas Kilikevičius _____
(*Position, Name, Surname*) (*Signature, date*)

Vinod Raj Begur Venkataraj. DESIGN AND ANALYSIS OF WANKEL ENGINE. *Master's* Final Project / supervisor assoc. prof. dr. Sigitas Kilikevičius; Faculty of Mechanical Engineering and Design, Kaunas University of Technology.

Research field and area

Kaunas, 2017. 71 p.

SUMMARY

The work deals with the design of the Wankel engine with an improved new apex seal. The motion study analysis is about the velocity at rotor vertex, contact forces and frictional forces. The computational fluid analysis is conducted to the designed model at 120bar pressure (power stroke) and the obtained results are exported to static FEA study. Static analysis is conducted to the rotor with different materials. The fatigue study is conducted to the rotor to check the life of the rotor by using Solidworks and theoretical calculations. Different types of rotary profiles are designed by manipulating K-factor. CFD analysis was carried out for a different rotary profile to check how K-factor influencing in Leakage and working chamber. The investigations conducted in the work justified the proposed new design solutions.

Keywords: *Wankel engine, Computational fluid analysis, Finite Element Analysis, Rotor, Fatigue Life, K-factor.*

Vinod Raj Begur Venkataraj. VANKELIO VARIKLIO PROJEKTAVIMAS IR TYRIMAS. Magistro baigiamasis projektas / vadovas prof. dr. Sigitas Kilikevičius; kauno technologijos universitetas, Mechanikos inzinerijos ir dizaino fakultetas.

Kaunas, 2017. 71 p.

SANTRAUKA

Darbe pristatytas Vankelio variklio projektavimas panaudojant patobulintą apekso sandarinimo konstrukciją. Judesio tyrimas. Atliktas variklio judesio tyrimas ir nustatyta rotoriaus viršūnės greitis, kontaktinės ir trinties jėgos. Skaičiuojamoji srautų analizė atlikta esant 120 bar slėgiui ir gauti rezultatai panaudoti atliekant rotoriaus stiprumo tyrimą baigtinių elemento metodo pagrindu. Rotoriaus stiprumas analizuotas vertinant skirtingas medžiagas. Rotoriaus ilgaamžiškumui nustatyti, atlikti nuovargio tyrimai naudojant Solidworks ir teorinius skaičiavimus. Manipuliuojant K faktoriumi, sudaryta keletas skirtingų rotorinių profilių. Kad nustatyti K faktoriaus įtaką darbinės kameros sandarumui, atlikta skaičiuojamoji srautų analizė skirtingiems rotoriniams profiliams. Darbe atlikti tyrimai patvirtino naujų projektinių sprendimų pagrįstumą.

Raktiniai žodžiai: *Vankelio variklis, skaičiuojamoji srautų analizė, baigtinių elementų analizė, Rotorius, nuovargis, K faktorius.*

TABEL OF CONTENTS

LIST OF FIGURES

LIST OF TABELS

INTRODUCTION

The Wankel engine is the type of internal combustion engine in which the engine uses rotary design to translate forces acting on the rotor into rotating motion as an alternative to using the reciprocating piston. It is also the same as a piston engine in which four strokes take place, but four strokes take place inside the housing.

The Wankel engine was the only internal combustion engine invented in the 20th century to go into manufacturing. Since the introduction of the Wankel engine, the engine is normally known as a rotary engine. German engineer Felix Wankel introduced this engine in 1929, he received his first patent and started a process in the 1950s at NSU Motorenwerke and in 1957 he built a working model. NSU then certified the engine idea to companies across the world, which have taken forward to advance the design.

Because of engine compactness in design, it has been mounted in a different vehicle such as automobiles, go-karts, personal watercraft, chain saws and racing cars etc.

Being a much-praised design in its earlier period, it was put behind by other engine models due to various reasons. Leakage in its apex seal is one of them, and, the research on apex seals are going on to reduce leakage problems. In this research, the thesis is focused on leakage problems between the apex seal and housing, and changing the rotor material to reduce the weight of the engine and comparing with the presently used materials [1].

The aim of this research is to design an internal combustion Wankel engine with an improved new apex seal. The major tasks raised to reach the aim of the thesis are:

1. the literature of the topic must be reviewed for the selection of the engine type and engine design. Design a basic engine model corresponding to all the calculation with kinematics and dynamics;
2. conduct a motion study with Solidworks motion to show the working model, contact forces, frictional forces between rotor housing and apex seal and comparing theoretical and experimental velocities of rotor vertex;
3. conduct computational fluid dynamic analysis of Wankel engine and considering a rotor as a main part for FEA analysing.
4. conduct a static FEA for different materials of rotor by importing results from CFD and calculate fatigue life.

5. design various geometries of triangular rotary profile by manipulating the K-factor to see the influence of the K-factor in Wankel engine.
6. conduct CFD on the various geometries of triangular rotary profile and to show how K-factor influence on a velocity of flow and leakage.
7. create 3D model and animation of the rotary engine by using Solidworks_2016 and 2D assembly drawings.

1. LITERATURE SURVEY OF WANKEL ENGINE

1.1. Definition of an engine

An engine is a mechanical device that can transduce one form of energy into useful mechanical energy or motion. If the engine converts fuel source to mechanical energy it is known as prime mover; if it produces kinetic energy from a pre-processed "fuel" (such as power, hydraulic fluid, and pressurized air), it is known as a motor. The device that produces energy in an automobile is known as the engine. A locomotive is also known as an engine.

The term "engine" originates from, an engine is a machine that transformed force into rotating motion. The term "gin" as in cotton gin is recognized as a form of the Olden French word *engin*, in turn from the Latin *ingenium*, related to *ingenious*.

In Early's 1900, human power was used to connect the simple engine like the capstan, windlass, or treadmill with ropes, pulleys, and block tackle arrangements, this power was conveyed and multiplied and used in cranes and aboard ships in Ancient Greece, and in mines, water pumps and siege engines in Ancient Rome [2].

1.2.Rotary engine

There are many designs invented to obtain motive power most of them are in rotary piston structure because the design structure was simple.

Identically, reciprocating engines have the following drawbacks:

- there is more vibration and noise due to more reciprocating parts, it leads to greater power loss as engine revolution increases;
- it creates noise and mechanism needs many parts because of intake and exhaust valve mechanism.

The rotary profile engine is excluded with valve mechanisms like intake and exhaust. The power is drawn from the rotating motion [3].

1.3.Evolution of rotary engine

The evolution of the rotary engine is explained below.

1.3.1. Rotary steam engine by James Watt

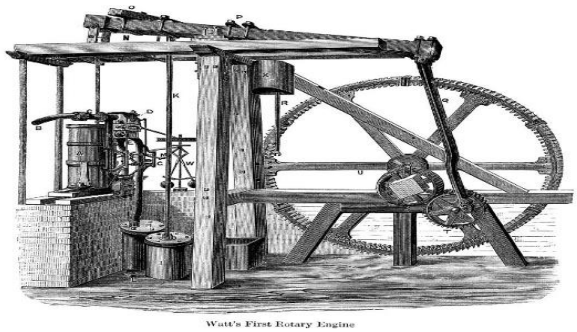

Fig 1.1- Rotary steam engine by James Watt [4]

The first rotary steam engine was introduced by James Watt in 1759. Though the engine is designed with a rotor, its rotating energy is extracted from steam pressure, it does not stay longer because of an airtightness problem [4].

1.3.2. Murdock's rotary steam engine

The Rotary steam engine was invented by Murdock in 1799. Wooden pieces were used to seal, improve airtightness and produced power for machine work and water pumps, but the engine does not satisfy the required airtightness and durability [5].

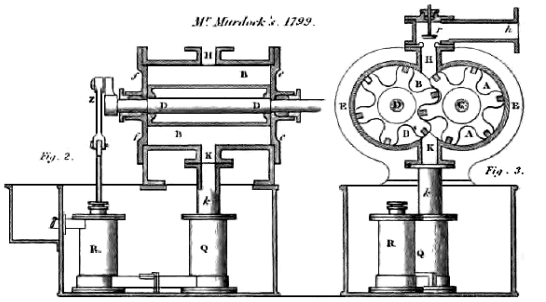

Fig 1.2- Murdock's rotary steam engine [5]

1.3.3. Behren's rotary steam engine

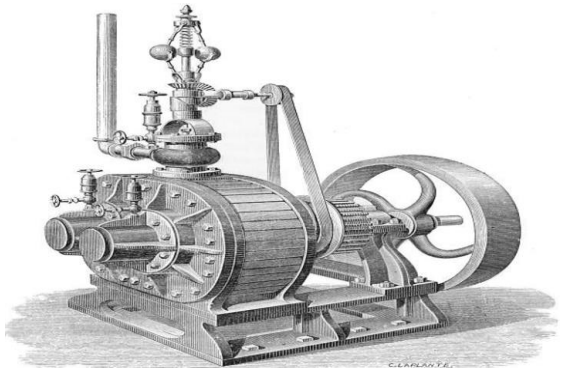

Fig 1.3- Behren's rotary steam engine [6]

This Behren's rotary steam engine was invented by Henry J, Behrens and patented in the year 1866 in USA. This is a new technique used in the engine. It has a hefty flywheel and fly-ball governor, which is placed on top of the casing, the steam coming through the vertical pipe at top left is controlled by a fly-ball. Behrens manufactured a rotary engine with improvised airtightness [6].

1.3.4. Colley's rotary steam engine

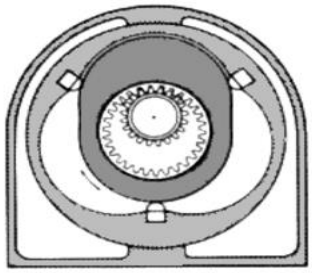

Fig 1.4- Colley's rotary steam engine [7]

In 1901 Colley introduced rotary engine, in the engine the outer and inner rotor rotates inside the engine. The inner rotor is designed by using the peritrichoidal curve and the outer rotor utilise the inner surface of the rotor. The engine was designed with 2-lobed inner epitrochoid and 3-lobed outer envelope in which the 2-lobed working inside the 3-lobed envelope [7].

1.3.5. Umpleby rotary engine

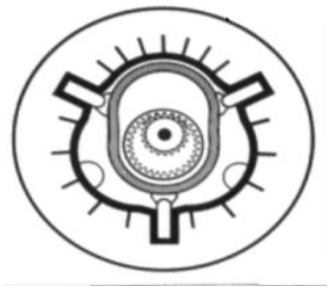

Fig 1.5- Umpleby rotary engine [8]

In 1908 Umpleby introduced rotary engine. Umpleby improvised the Colley's steam engine this was the first internal combustion engine [8].

1.3.6. The rotary engine by Wallinder and Skoog

Wallinder and Skoog introduced the rotary engine in 1923. A Swedish patent was granted to them in respect of a true piston thermal engine with toothed meshing, enveloping interior hypocycloid and internal five pointed rotors with a 5:6 rotation ratio which could be used as either 2 or 4 stroke internal combustion engine [7].

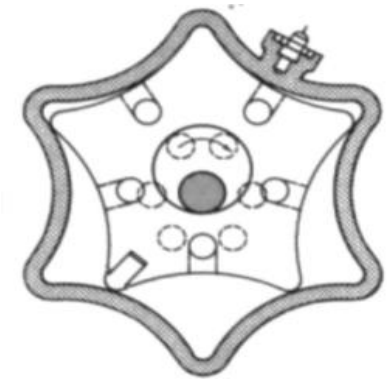

Fig 1.6- The rotary engine by Wallinder and Skoog [7]

1.3.7. The Maillard's rotary compressor

In 1943 Maillard introduced compressor by applying the steam rotary engine theory. Hypotrochoid curve is used for the rotor and its outer envelope for its inner surface of the housing. This rotary profile with 2:3 ratio and internal hypocycloid surface chamber [7].

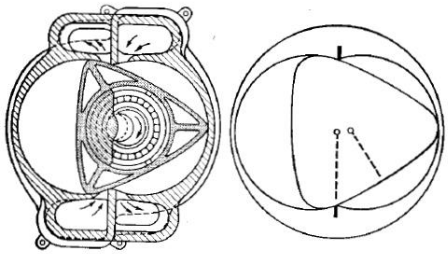

Fig 1.7- The Maillard's rotary compressor [7]

1.3.8. Wankel engine

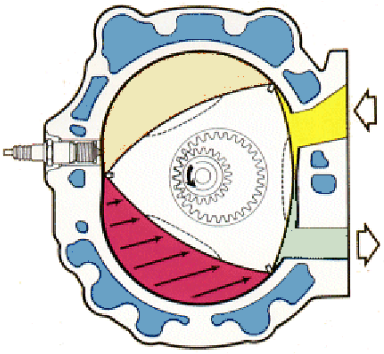

Fig 1.8- Wankel engine [12]

The Wankel engine is also one of the internal combustion engines it uses eccentric rotary design to convert forces acting on a rotor to rotating motion. The Wankel engine has many advantages like effortlessness, softness, compactness, and a high power-to-weight ratio. The four-stroke cycle takes place inside the housing and a rotor, that is similar in shape to a Reuleaux triangle with apex sides inside the rotor housing and somewhat flatter in shape.

- The first prototype of Mazda's wankel was 40A in 1959, it is the single rotor engine. The engine has a vibrating problem, rotor seal and the oil consumption problem seen in this engine.
- L8A is the first Mazda Cosmo prototype with 798 cc and had two rotors. It is exposed in 1963 in the Tokyo motor show. To reduce vibration in the rotor apex seal the hollow cast iron apex seals were used.

- 10A (1967-1973) series was a first wankel production in Mazda, appeared in 1965. It was a two-rotor design, with each displacing 491 cc for a total of 982cc. This engine featured the mainstream rotor dimensions with a 60 mm (2.4 inch) depth.
- 13A (1970-1972) was designed especially for front wheel drive applications. It had two rotors with 655 cc, this was the only production wankel with different rotor dimensions.
- 12A (1970-1985) is an "elongated" version of the 10A the rotor radius was the same, but the depth was increased by 10 mm (0.4 in) to 70 mm (2.8 in). It has two rotors with 573cc each.
- 13B (1973-2002) is the most commonly produced engines. It was the basis model for all future Mazda Wankel engines, and the engine was mostly used for over more than 30 years. The 13B has totally different to the 13A.
- Renesis (2004-2013) 13B-MSP (Multi-Side Port) – these are the newly designed model with multi side port started production in 2003 Mazda RX-8, is an upgrade of the previous 13B [10-13].

1.3.9. Problems with Wankel engine

The most of the problems in Wankel engine are leakage problems that lead to lower fuel efficiency. Apex seal is one of the first parts to fail in engine otherwise it uses to be consistent engine design. In fact, the majority of people say apex seal is the weakest part of a Wankel engine. The rotor is one of the main part in Wankel engine it is a triangle in shape and made up of cast iron. The apex seal is placed between rotor and housing, the only part moving in the engine is apex which is in direct contact with the housing. A faulty apex seal can cause a lot of problems. So, some points listed below [14].

- **Rotor sealing:** the rotor sealing is the one of the problems in engine housing. In engine housing, each stroke takes place in different temperature in the chamber section which influences to leak due to more pressure.
- **Apex seal lifting:** In the engine housing, there will be so many forces acting on the apex seal the centrifugal force is mainly considered to make contact between the housing and apex surfaces a firm seal. Due to light load operation when an imbalance of centrifugal force leads to a gap between the apex seal and trochoid housing which may directly effect in gas leakage.
- **Slow combustion:** Long, thin and moving combustion chamber make the process of combustion slower.

- **Bad fuel economy:** The main reasons for the Bad fuel economy are sealed leakages, with poor combustion behaviour and mean effective pressure at part load, low rpm. The engine running at constant speed leads to burn off more fuel consumption [14].

1.4. Apex seal

In the early 1960s the biggest problem with the rotary engine, researchers and development engineers faced the rotor housing sliding surface. Frictional vibrations of the apex seals. Inadequate lubrication of the trochoid, the natural frequency of the sealing elements and the coefficients of static and kinetic friction could also aggravate it [15].

1.4.1. Two-piece metal seal

A high wear resistant, cast iron apex seal replaced the carbon-compound design in the mid-1970s. This was made possible by the new pinpoint-porous chrome-plating on the trichord's sliding surface, which greatly improved housing and apex seal lubrication. The rubbing tip of the seal is crystallized in the form of carbides, a process called electron beam chill hardening. The treatment gives the seal tip an almost ceramic-like composition. The change of the seal materials allowed a new two-piece seal design with the main body and a triangular corner piece, greatly enhancing gas-sealing performances. The seal thickness was halved to 3mm [15].

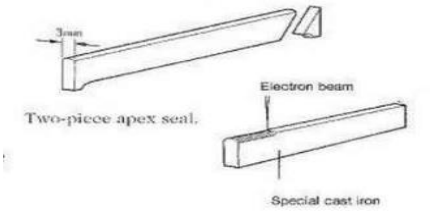

Fig 1.9- Two-piece apex seal [15]

1.4.2. Top-cut apex seal

Adopting a top-cut design with an extended main seal piece reduced gas leakage area at one end of the apex seal, where it is divided into two pieces [15].

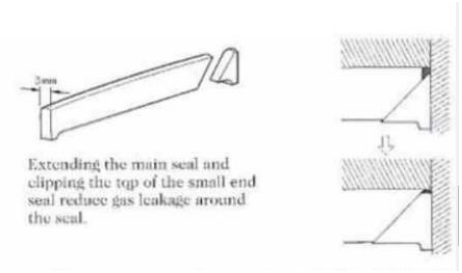

Fig 1.10- Top-cut apex seal [15]

1.4.3. Three-piece apex seal

These apex seal thickness has been further reduced to 2mm. The previous two-piece configuration has been replaced with a new three-piece design. The main seal is divided, laterally and at an angle, into upper and lower pieces, while retaining the triangular end piece. The top piece now slides up and down vertically on the lateral and angled contact surface with the lower element. Tighter gas sealing is the aim of the design. The spring corner seals central is filled with heat-resistant rubber material, eliminating a minute leakage from the source [15].

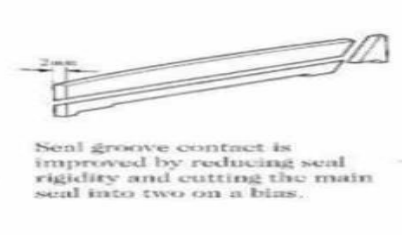

Fig 1.11- Three-piece apex seal [15]

1.4.4. New two-piece apex seal (2003 RX-8 RENESIS)

New two-piece apex seal of acicular cast iron with very low carbon content is adopted in the RENESIS two-rotor engine, the seat's height is lower than the top piece of the previous three-piece design, 4.5mm versus the three-piece top piece's 4.8mm. The digitally controlled, electron beam chill-hardening process results in a deeper and more uniform hardened area at the tip of the seal. The apex seal is crowned and its tip is rounded so that it follows the trochoid sliding surface up to the engine's higher peak revolutions of 9000rpm [15].

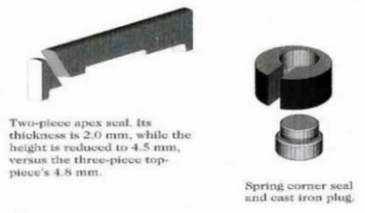

Fig 1.12- New two-piece apex seal [15]

1.4.5. Problems with Apex seal

The problems of apex seal are mentioned earlier in 1.3.9, there is a problem in apex seal leakage when the pressure acts on the apex seal tries to move, then it creates gap between the apex seal and housing. Below figure 1.13 shows the apex seal with gap and gas leakage.

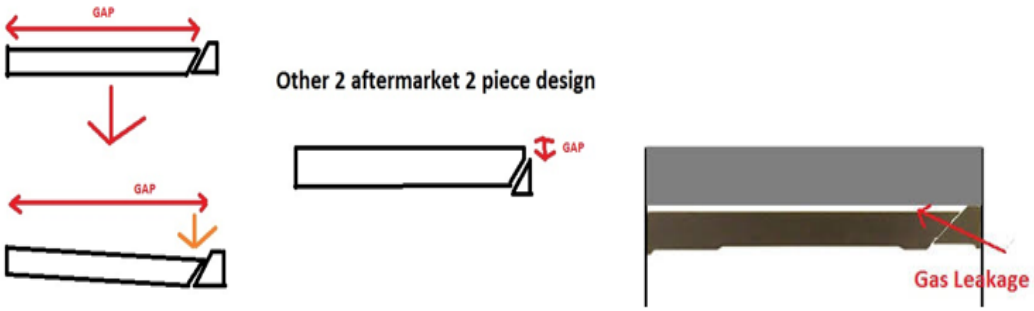

Fig 1.13- Problems in apex seal.

1.5. Engine Kinematics (Motion study)

The work of Centenaro Stefano and Furlan Ismaele, “Wankel engine”. This paper gives more information how the Wankel engine is designed, more about the kinematic and dynamic study of Wankel engines. It is clearly explained how to conduct motion study, what are the formulas used to determine the velocity of rotor vertex [16].

$$v = \frac{\omega}{3}\left(9e^2 + R^2 + 6eR\cos {}^{2}/_{3}\,\alpha\right)^{1/2}, \tag{1.1}$$

The work of Zhang, De-Lou; Wu, Yu-ting; Wang, Jing-Fu; Du, Chun-Xu; Chen, Xia; Ma, Rui; and Ma, Chong-fang, "Theoretical Study of Seal Spring in a Wankel Compressor" (2016). International Compressor Engineering Conference. The paper shows how the force acting on the apex seal due to spring, what are the forces acting on the spring and which type of study is used to find the frictional forces due to spring into action. The apex spring plays a vital role in compacting internal surface of the housing, which may lead to plastic deformation and abrasion. It is important to research the force acting on the apex seal due to springs and motion of apex seal. A schematic drawing of a plate spring, used in Wankel engine is shown in a figure. The black line represents the original state and red one is operating state of the apex seal [17].

The stress condition is worst in the spring, while the seal is along the short axis. Below figure shows the component force of spring are zero in the horizontal direction and resultant forces F_R is worked as follows:

$$F_R = F_r + F_{sl} + F_{gr} + F_m, \tag{1.2}$$

Where, F_r-the radial inertial force of seal; F_{gr}-back pressure; F_{sl}- force of spring; F_m- inertial forces

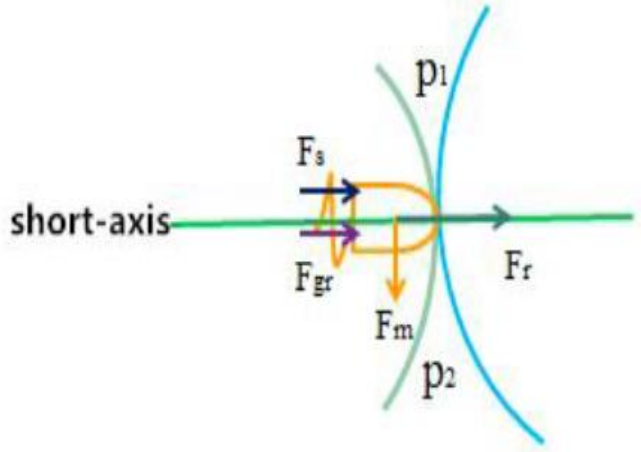

The free body diagram of apex spring and apex seal.

$$F_r = \frac{W}{g}\omega^2\left(\frac{R}{9} + e cos\frac{2}{3}\alpha\right), \tag{1.3}$$

Where W-the weight of the apex seal; g-acceleration of gravity; ω- angular velocity of the eccentric shaft; R- the centre of gravity of seal and rotor centre; e-eccentricity.

$$F_{gr} = l\left(\frac{b}{2} + asin\phi\right)(P_1 - P_2), \quad (1.4)$$

Where l-length of the seal; b- width of the seal; a radius of the apex seal; ϕ- leaning angle

$$F_r = \frac{W}{g}\omega^2\left(\frac{R}{9} - e\right) \quad (1.5)$$

By using the above-given formulas, the force acting on the apex seal is calculated and the calculated results are used to run a motion study of the Wankel engine to find the velocity and acceleration at rotary vertex [17].

1.6. Computational fluid dynamics

Computational fluid dynamics is a part of fluid mechanics that uses numeric analysis and data structure to solve and analyse problems that involve fluid flows.

There are so many research papers on CFD Wankel engine. There are few papers which are related to my research work which has been listed below [18, 19].

The work of Albert Boretti on Modelling unmanned aerial vehicle, jet ignition wankel engines with CAE/CFD. The paper presents some details of the CFD modelling of a novel design where jet ignition devices replace the traditional spark plugs for a faster and more complete combustion. The CFD is conducted for different speed with different pressures. The paper proposes the procedure for conducting CFD and how the results are compared and so on [20].

The work of ZHAO Yuqiao, Loh Wai Lam, and Lee Thong-See on CFD Simulation of a Pump with Wankel Engine Geometry. The paper explains the contact between the internal profiles and the trochoid of the rotary engine. The theme of this paper to study the possibility of applying geometry of the Wankel Rotary Engine to pump design and the pressure field with the compression compartment and ports was studied by CFD code solver [21].

The work of Baowei Fan, Wenming Yang, Hui An, Xia Shao & Hong Xue discovered the Effects of different parameters on the flow field of peripheral ported rotary engines. The paper explains how the performance of the rotary engine is influenced by the flow field. The work contains a detailed mathematical model and simulated software FLUENT to investigate the flow field in a peripheral ported rotary engine, the flow in the combustion chamber was studied and the effect of the 3 major parameters

of the field in the combustion chamber like speed, intake shape and intake angle was also investigated [22].

The work of Chol-Bum M. Kweon, Army Research Laboratory on Fuelled Rotary Engine Combustion Technologies explains the details about the present understanding of combustion chamber design, fuel spray, apex, side seals, and how to conduct computational fluid dynamics in the engine and working of the engine combustion chamber. In this paper, it is clearly mentioned the state of the art rotary engine combustion technologies, to gain insight into technology gaps that need further research and development [23].

1.7. Fatigue study

The fatigue study is conducted to predict the life of the model. It is observed that repetitive loading and unloading weakness the strength of objects over time, even when the induced stress is considerably less than the allowable stress limits is known as fatigue; each cycle of stress acting on object reduces the strength of the object to some extent. After several cycles, the object loses his strength, then it fails. Fatigue is the main cause of the failure of the product, especially the product is made up of metals. For examples of failure due to fatigue include rotating machinery, nuts, and bolt.

The work of Deepan Marudachalam M. G, K. Kanthavel and R. Krishnaraj on Optimization of shaft design under fatigue loading using Goodman method, International Journal of Scientific & Engineering Research, paper provides information to calculate the infinite life cycle and to conduct the fatigue study of the given model [24].

The work of R.A. Gujar and S.V. Bhaskar on shaft design under fatigue loading by using Goodman method explains the details of fatigue study, mechanical properties of the materials, and uses of the SN curve for life evaluation and how to calculate or design the infinite life of the given object. The paper clearly explains the uses of fatigue study and how to evaluate the number of cycles to obtain infinite life [25].

1.7.1. Fatigue life evaluation

These four theories are used for the prediction of failure from fluctuating load.

a) Soderberg $$\frac{\sigma_a}{\sigma_e'} + \frac{\sigma_m}{\sigma_y} = 1 \quad (1.6)$$

b) Goodman $$\frac{\sigma_a}{\sigma_e'} + \frac{\sigma_m}{\sigma_u} = 1 \quad (1.7)$$

c) Gerber $$\frac{\sigma_a}{\sigma_e'} + \left(\frac{\sigma_m}{\sigma_u}\right)^2 = 1 \quad (1.8)$$

d) Morrow $$\frac{\sigma_a}{\sigma_e'} + \frac{\sigma_m}{\sigma_f} = 1 \quad (1.9)$$

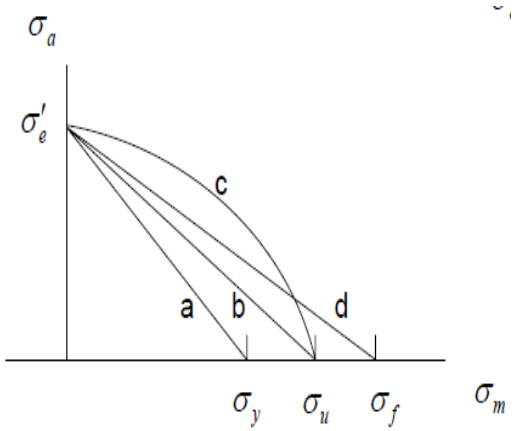

σ_y=yield stress, σ_u=ultimate stress, σ_f=true fracture stress, σ_a- Alternating stress and σ_e'- Effective alternating stress [26, 27].

1.7.2. Use of empirical curves for an infinite life design

Use a curve such as the Goodman with $\sigma_e' = \sigma_e$ The endurance limit, N_f is infinity.

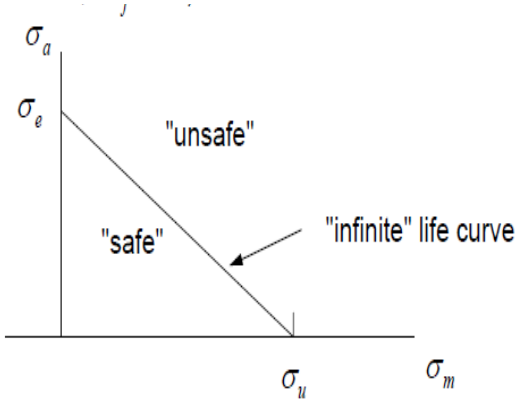

Any combination of mean and alternating stress that are to the left of the curve are deemed safe, those to the right are not [26, 27].

1.7.3. Calculation for infinite life

When the model is to be designed for infinite life, the endurance limit becomes the criteria of failure. The amplitude stress on the such components should be less than the endurance limit to withstand the infinite number of cycles. Such a component is designed with the help of solving equation [24, 25].

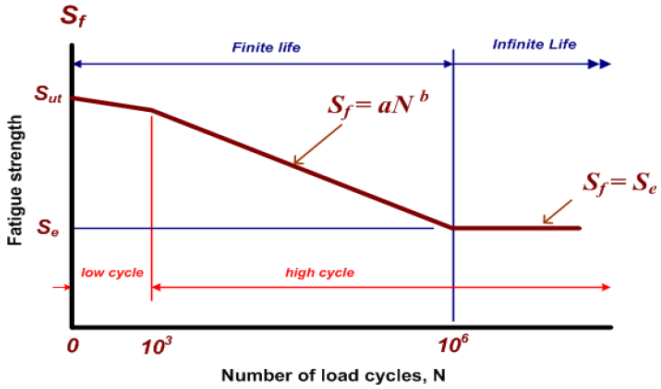

Fig 1.14- S-N curve [25]

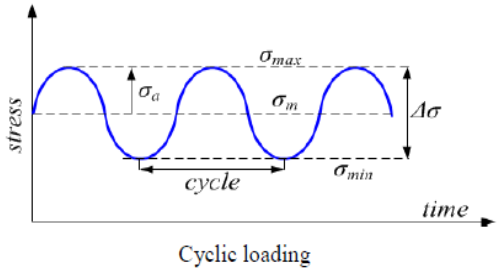

Cyclic loading

$$\sigma_{mean} = \sigma_m = \frac{\sigma_{max} - \sigma_{min}}{2} \tag{1.10}$$

$$\sigma_{alternative} = \sigma_a = \frac{\sigma_{max} - \sigma_{min}}{2} \tag{1.11}$$

$$R = \frac{\sigma_{min}}{\sigma_{max}} = 0(unidirectional\ loading) \tag{1.12}$$

High fatigue life is achieved (N> 1000cycles) and infinity life if (N>10^6)

Equation if line $y = ax + c$

Number of cycles from S-N construction

$$logS_f = a(logN_f) + c$$

$$S_f = \overline{AO} = \frac{\overline{XD} * \overline{OC}}{\overline{DC}}$$

$$S_f = \frac{\sigma_a * S_{ut}}{S_{ut} - \sigma_m} \tag{1.13}$$

$$\log_{10}(N_f) = \frac{(6-3)(\log_{10}(0.9S_{ut}))-\log_{10}(S_f)}{\log_{10}(0.9S_{ut})-\log_{10}(S_e)} + 3 \quad (1.14)$$

$$S_f - fatigue\ strength$$

$$S_e = S'_e * k_a * k_r * k_{sz} * k_{sf} \quad (1.15)$$

$$S'_e = 0.4S_u\ for\ S_u < 400Mpa = 160MPa\ for\ all\ other\ values\ of\ S_u$$

$$S'_e\ values\ depend\ on\ the\ materials$$

N_f-gives the number of cycles to failure [24]

1.8. Effect of K-factor (leakage and working chamber)

The work of Michael Irvin Resor, Computational investigation of rotary engine. This paper explains about the model creation and numerical settings for the validation study, with diesel engine, rotary engine model creation and a case study for selecting the optimal K-factor, using pressure rise rate, peak pressure and indicated power as selection criteria [28].

The work of Chiu-Fan Hsieh & Hao-Yu Cheng, effects of various geometric designs of K-factor, International journal paper. The research on k-factor shows that what are the effects of changing the value of k-factor and how they are influenced. In this study, the paper discussing what are the methods used to design different profiles of k-factor and how to analyse the leakage problem in design [29].

Mathematical model

The theoretical curve of the rotary engine housing is most commonly epitrochoidal assuming the rolling circle $\Sigma_r$with radius ρ_r followed another fixed circle Σ_b with radius ρ_b rolling an internal tangent, then when, $\rho_r > \rho_r$, $\rho_r = 1.5\rho_b$, and α=3β,

Where,

$$x_1 = c\cos\alpha + \frac{3kC^2}{\rho_r}\cos\beta \quad (1.16)$$

$$y_1 = c\cos\alpha + \frac{3kC^2}{\rho_r}\cos\beta \quad (1.17)$$

The housing envelope is created by using below equations.

$$x_1 = c\cos 2^{\gamma} + ccos(\alpha + {}^{\gamma})\frac{3kC^2}{\rho_r}\cos\left(\frac{\alpha}{3} + {}^{\gamma}\right), \quad (1.18)$$

$$y_1 = c\cos 2\gamma + ccos(\alpha + \gamma)\frac{3kC^2}{\rho_r}\cos\left(\frac{\alpha}{3} + \gamma\right), \quad (1.19)$$

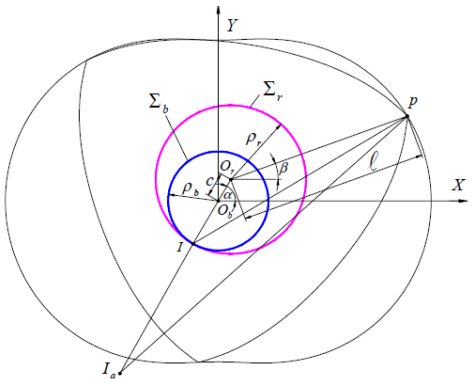

Fig 1.15- Generation principle of profile [29]

The profile is generated by using the above equation to the different types of k-factor. To conduct fluid analysis, there are different types of governing equation is shown. Turbulence is considered for using a standard *k*-ε two-equation model. Boundary conditions are used to compute the flow simulation. Three different profiles are designed to do flow simulation in 2D by using Ansys gambit software. The procedure is carried out like geometry generating, meshing and solving [29].

From Literature survey,

- In a nutshell, Firstly, the engine is to be designed like the existing one (like 13B and Rensis). But concentrating on major improvements with new apex seal and the research on the usage of aluminium material for rotors to reduce the overall mass;
- secondly, research papers used to study kinematics, CFD and Fatigue provides the information to conduct the analysis on wankel engine and also to derive all the basic parameters used in engine with the necessary calculations;
- finally, the survey of K-factor provides information how to design different rotary profiles, what are the boundary condition to be considered and information to conduct CFD.

2. DESIGN OF WANKEL ENGINE

2.1. 3-D Model of Wankel engine

3-D model of wankel engine is designed by using Solidworks 2016 the figure 2.1 shows the designed model of Wankel engine.

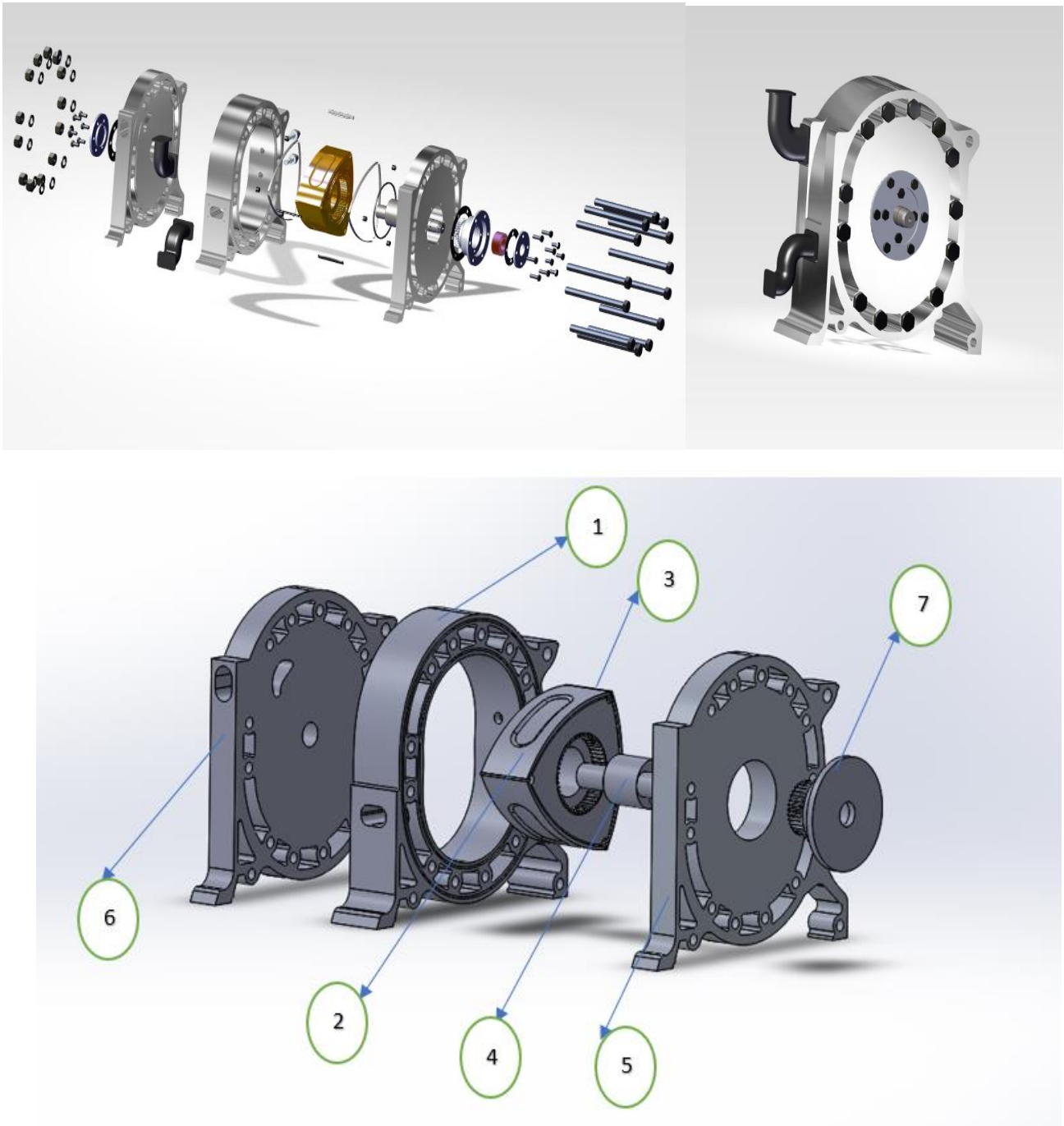

Fig 2.1- 3D model of the Wankel engine (using Solidworks 2016).

The design is a combination of existing Renesis and 20B engine. In this design, the main parts are (Rotor, Housing, Eccentric shaft, Back plate, Front plate and apex seal). The engine provided by a single rotor. Thus, one rotation of a rotor is same as one planetary cycle and one rotation of the rotor (360degree) is equal to 3 rotations of the eccentric shaft with (1080degree). For each rotation of the rotor is a combination of 4 strokes from intake to exhaust. Each of the four strokes from suction to exhaust takes place in the 1080/4=270degree rotating angle of the eccentric shaft, which is quite different from the 4-stroke reciprocating engine. In this planetary rotation engine, since the remaining two chambers also operate with the phase difference of 360 degrees of the eccentric shaft rotation, each rotation of eccentric shaft the combustion stroke place at every rotor face [30, 31].

1. **Rotor Housing-** the inner surface of the housing curve is obtained by a Peritrochoid equation. There are so many passages on the outer surface to cool the engine. Further on rotor housing is provided with spark plug holes, an exhaust port, etc;
2. **Rotor-** the rotor works like the piston and connecting rod of a reciprocating engine, the forces acting on the rotor is converted into rotary motion. The rotor acts as an intake-exhaust valve as it rotates. The rotor is provided with an apex seal and side seals. The rotor gear and bearing are incorporated in its centre. The shape of the rotor is based on a K-factor and the influence of the rotor housing. A recess is provided on each rotor face it is used to increase the chamber volume and it is known as rotor recess;
3. **Apex seal -** the apex seal is the main components which act as a sealing between rotor and rotor housing to keep the pressure inside the different chambers.
4. **Eccentric shaft-** the rotor journals are eccentric to the centre of rotation of the output shaft by the eccentricity e of the trochoid. The diameter of the journal is considered from the phasing gear design with respect to eccentricity e.
5. **Side housing -** the side housing is provided with an intake port. And at the centre, there is a hole for the eccentric shaft and for phasing gear. The side housing has sliding surfaces.
6. **Phasing gear -** The phasing gear is designed with an external gear fixed to the side housing and the internal gear installed in the rotor, corresponding respectively to the Peritrochoid generating base circle and rolling circle. The rotor gear and rotating shaft are designed in 1:3 ratios and stationary gear and phasing gear are designed in 2:3 ratios for the pitch diameter.

2.2. Engine parameters:

As explained in the introduction the primary goal is to design a Wankel engine. To design rotor and housing we require some engine parameters such parameters are shown below in the table [7,32].

Table 2.1- Basic Dimensions of Engine.

VH (cm^3)	250
***e* (mm) - eccentricity**	10.9
***R* (mm) – generating radius**	80
***b* (mm) -width**	55
K*-factor =*R/e	7.34
φ_{max}-Maximum lean angle	24.12
Weight (Kg)	16.1

Pressure calculation for 250 cm^3, 1 rotor Wankel engine:

For One-Rotor engine, specification for 250 cm^3

The formula for displacement is

$$D = 3\sqrt{3}eR_1bN \quad (N \text{ is number of rotor=1}) \tag{2.1}$$

$$D=3*1.732*10.9*80*55*1$$

$$D=249.192\ cm^3 \approx 250\ cm^3$$

2.3. Peritrochoid (Housing)

The basic curve is obtained by Peritrochoid equation, the rotor housing is designed by using the curve generated by the equation.

2.3.1. Peritrochoid Equation

The Peritrochoid is the locus of the tip point *P* of an arm fixed on the rotating circle *B* in diameter *q*, it rotates with the periphery of the circle *A* in Radius *P* as inscribed. Then, to derive the cure for housing given by the organizes of point *P* (*x*, *y*) in the organizes *x*, *y* of the centre of base circle *A* [32].

$$x=e\cos\alpha+R\cos\beta \quad (2.2)$$

$$y=e\sin\alpha+R\sin\beta \quad (2.3)$$

therefore, e: distance between the centre base circle A, and rolling circle B

R: length of rolling circle B

α: angle of rotation of revolving circle B

β: circle B rotating angle

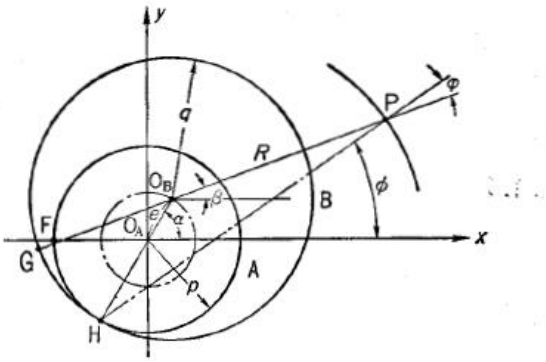

Fig 2.2- Generating the Peritrochoid [32]

From fig 2.2, point F on fixed circle A and point G revolving circle B the point of interaction between the circles when α=0 and β=0. From the relation, $FH=GH$

$$q\,(\alpha-\beta)=p\alpha$$

$$\beta=(1-p/q)\,\alpha$$

The above equation shows the angle of rotation α of the revolving circle around the base circle A and β on its axis are in a proportionate relation.

$$p/q=(m-1)/m,$$

Peritrochoid equation can be written as

$$x=e\cos\alpha+R\cos\,\alpha/m, \quad (2.4)$$

$$y=e\sin\alpha+R\sin\,\alpha/m, \quad (2.5)$$

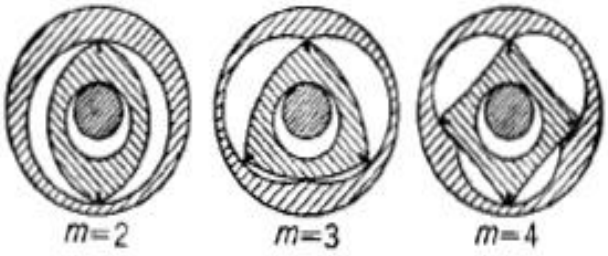

Fig 2.3- Configuration Peritrochoid and an inner surface [32]

From the fig 2.3 shows the configuration of the curves where m=2, 3 and 4, respectively.

The rotary engine uses the trochoidal constant m=3, which is expressed, as

$$x=e\cos\alpha+R\cos\alpha/3 \quad (2.6)$$

$$y=e\sin\alpha+R\sin\alpha/3 \quad (2.7)$$

Where, e is the amount of eccentricity and generating radius R.

Fig 2.3 shows the trochoid constant K and the configuration of the trochoid when the working volume is taken as constant [7, 32].

2.3.2. Calculations for rotor housing

The above equations and procedure are used for deriving the peritrichoidal curve (rotor housing), the curve of Wankel inner housing is obtained by using Solidworks spline curve options. The equations used and sketches are shown below.

$$Xt=(80*\cos(t)) +(10.9*\cos(3*t)) \quad (2.8)$$

$$Yt=(80*\sin(t)) +(10.9*\sin(3*t)) \quad (2.9)$$

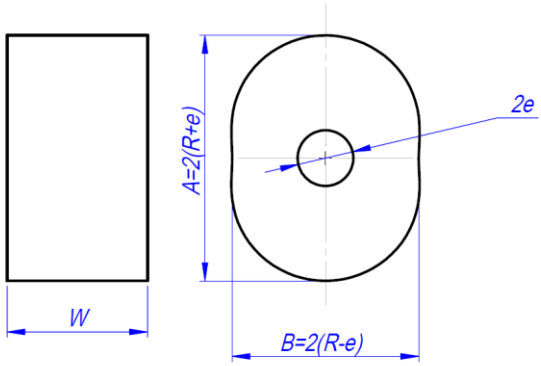

Where, *R*-radius of housing-80 mm

e-ecentricity-10.9 mm

W-width-55 mm

Therefore, $A=2(R+e)$ (2.10)

A=181.8 mm

$B=2(R-e)$ (2.11)

B=138.2 mm

In housing design, I equated equation of the peritrichoidal curve in the Solidworks part model with equation driven spline curve option.

2.4. Inner envelope of Peritrochoid

To design rotor the inner envelope should be created to create the inner profile, the Peritrochoid drawn by the Peritrochoid fixed on Circle *A* when it rotates along with the inner profile of the housing of the inactive Circle *B* as inscribed. From the fig 2.4 the inner line of this pattern is known to be the inner envelope [32].

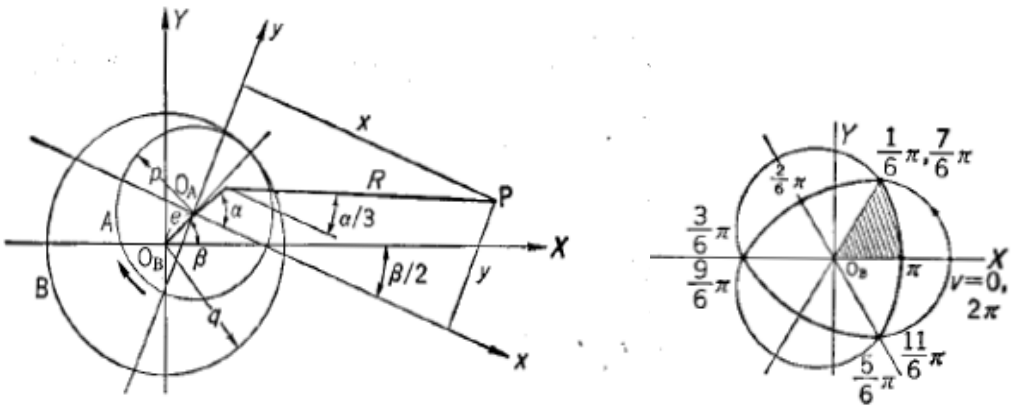

Fig 2.4- Generation of the inner envelope of Peritrochoid [32]

2.4.1. Equation and calculation of rotor

When *x*-*y* coordinate system rotates as fixed to the revolving circle *A*, the following between the *x*-*y* and *X*-*Y* coordinate will be recognized [32].

$$X=e\cos\beta + x\cos\beta/2 + y\sin\beta/2$$

$$Y=e\sin\beta + y\sin\beta/2 + y\cos\beta/2$$

The equation for inner envelope is given as,

$$X = R\cos 2v + \frac{3e^2}{2R}(\cos 8v - \cos 4v) \pm e(1 - \frac{9e^2}{R^2}\sin^2 3v)\text{^}1/2\ (\cos 5v + \cos v) \quad (2.12)$$

$$Y = R\sin 2v + \frac{3e^2}{2R}(\sin 8v - \sin 4v) \pm e(1 - \frac{9e^2}{R^2}\sin^2 3v)\text{^}1/2\ (\sin 5v - \sin v) \quad (2.13)$$

This function is cyclic functions with the period of 2π.

$$v = \frac{1}{6}\pi - \frac{1}{2}\pi,\quad \frac{5}{6}\pi - \frac{7}{6}\pi,\qquad \frac{3}{2}\pi - \frac{11}{6}\pi$$

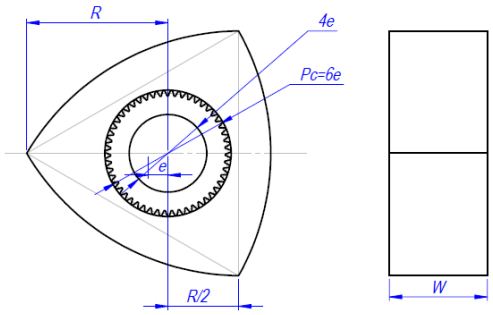

Where, *R*- distance of each rotor vertex=80mm

e- eccentricity=10.9 mm

Pc- pitch circle diameter=6*e*

W- width of the rotor=55 mm

4*e*- diameter of the eccentric shaft journal=43.6 mm

2.5. Angle of oscillation

The angle of oscillation that is curved by the creating radius of the Peritrochoid and the normal of the trochoid.

2.5.1. Maximum angle of oscillation

The maximum value of the angle of oscillation is known as the maximum angle of oscillation. The maximum angle of oscillation φ_{max} is presented by α, φ_{max} can be calculated by using the equation below [7, 32].

$$\sin \varphi_{max}=3e/R \quad (2.14)$$

Calculation of φ_{max},

$$\sin \varphi_{max}=3/K \quad (2.15)$$

$$\sin \varphi_{max}=3/7.34$$

$$\varphi_{max}=24.12 \text{ degrees}$$

2.6. Eccentric shaft

The eccentric shaft is shown in fig 2.5, the shaft of the rotary engine is like the crankshaft of the piston engine in its function. It produces the rotating motion by receiving the pressure acting on the rotor journal eccentric to the centre of the eccentric shaft to the output. It completes 3 rotations to the one rotation of the rotor, it is 3 times faster than the rotor. A flywheel and v-belt pulley is fitted to its ends. The basic geometric dimensions of an engine affect the determination of the dimensions of output shaft including the rotor, in other words, the eccentric shaft system.

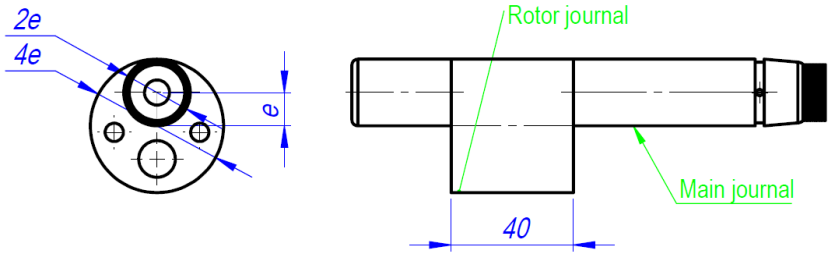

Fig 2.5- Eccentric shaft.

Therefore,

e- eccentricity = 10.9 mm

2*e*-diameter of shaft = 21.8 mm

4*e*-diameter of rotor journal = 43.6 mm

Width of Rotor journal = 40 mm

2.7. Design of gears

The phasing gears, consisting of the stationary external gear fixed to the side housing (which also functions as the housing for the main bearing), and the internal gear installed inside on one side of the rotor, are automatically determined by the basic dimensions of the engine, especially as to trochoid eccentricity (*e*) and trochoid generating (*R*) [32].

Therefore, these phasing gears are generally designed as shifted spur gears, in which case the mating equation for the shifted internal gear are expressed as,

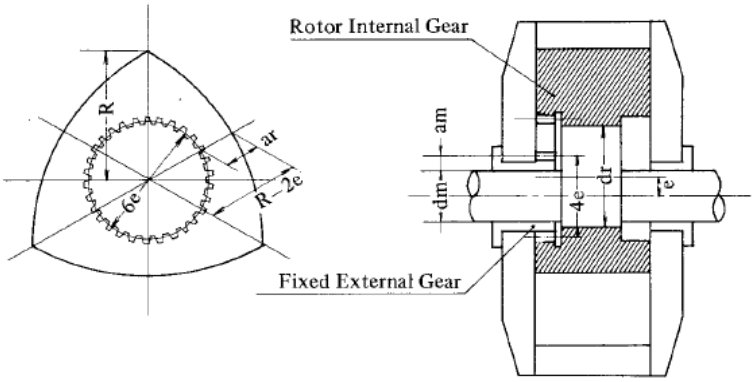

Fig 2.6- Rotor and Housing gears [32]

where, 2*p*=4*e* and 2*q*=6*e* express the diameter of the pitch circles of the external gears fixed to the side housing and of the internal gear of the rotor, respectively.

From the fig 2.6 above, we get:

$$a_m = 2e - \frac{dm}{2} \geq 3e - \frac{d_r}{2} (d_r \geq d_m + 2e), \tag{2.16}$$

Where the value of a_m is properly selected according to the tooth number of the fixed gear and its module.

Therefore, the eccentricity (*e*), once determined will inevitably the minimum values of the diameter dm of the main bearing journal and of the diameter d_r of the rotor bearing journal.

Since a_r is the distance between the pitch circle diameter of the rotor internal gear and the arc shaped rotor contour, the proper value should be determined in accordance with number and size.

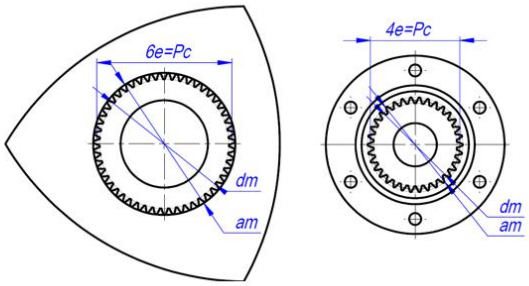

Phasing external gear

Centre distance of mating gear A=e=10.9 mm

Pc: Pitch circle diameter is 4e =45 mm

a_m: Addendum Pc+3=48 mm

d_m: Dedendum Pc-3=41 mm

M: Module $A = \frac{Z_2 - Z_1}{2} M$ =1.5

Z_1: Number of teeth of the external gear= 34

α: cutter pressure angle= 20 degree

Rotor internal gear

Pc: Pitch circle diameter is 6e =67.5 mm

a_m: Addendum Pc+3=70.5 mm

d_m: Dedendum Pc-3=63.5 mm

M: Module $A = \frac{Z_2 - Z_1}{2} M$ =1.5

Z_2: Number of teeth of the external gear= 51

When using equations, letting the centre distance(A) between the mating gears equal the eccentricity of the rotor journal, that is, A=e, and the ratio of the tooth number of the stationary gear to that of the rotor gear Z_1: Z_2= 2:3.

2.8. Apex seal

The apex seal is placed at each corner of the rotor it acts as a sealing component between the rotor and rotor housing [4,33].

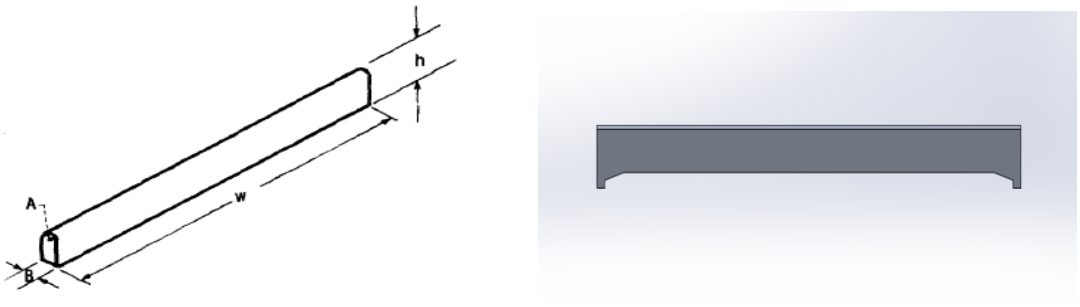

Fig 2.7- Apex seal.

The width of the apex seal always should be

$$B \geq \frac{6ea}{R} \tag{2.17}$$

$$B \geq \frac{6 * 10.9 * 1}{80}$$

$$B \geq .8175 \text{ mm}$$

Therefore, *B*- width of the apex seal =2 mm

A-radius of the apex seal =1.5 mm

W- Length = 55 mm

H- Height of the apex seal is =8 mm

Calculation of forces on apex seal

In the rotary engine, the seal continues moving in the same direction so the forces acting on the apex seals are calculated. The difference between the maximum and minimum speeds is relatively little. The calculation will be helpful to the CFD and motion study to conduct an analysis.

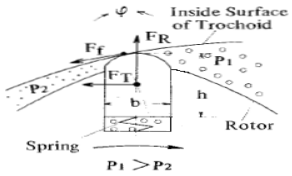

$$F_R = F_r + F_{gr} + F_s,$$

Where, F_R: resultant force applied to the seal in the direction of the radius

F_r: inertia force applied to the seal in the direction of the radius

F_s: force applied by the spring in the radial direction

F_{gr}: force by gas pressure in the direction of a radius

The pressing force applied by gas pressure equation when $P_1 > P_2$

$$F_{gr} = l\left(\frac{b}{2} + asin\varphi\right)(P_1 - P_2) \tag{1.4}$$

Where, P_1: gas pressure inside high pressure side working chamber = 120 bar

P_1: the gas pressure inside low pressure side working chamber = 1 bar

a: radius of the round top surface of apex seal = 1.5 mm

b: width of apex seal = 2 mm

l: axial length of apex seal=55 mm

φ: leaning angle = 24.12 degrees

$$F_{gr} = 0.055\left(\frac{0.002}{2} + 0.0015sin24.12\right)(120 - 1)$$

$$F_{gr} = 1765.39\ N$$

The resultant force can be given by

$$F_r = \frac{W}{g}\omega^2\left(\frac{r}{9} + ecos\frac{2}{3}\alpha\right) \tag{1.3}$$

Where, *r*: distance between the centre of the rotor and the centre of gravity of the apex=77 mm

W: weight of the apex seal=5 g

e: eccentricity of the eccentric shaft=10.9 mm

α: angle of oscillation of the eccentric shaft= 0, 270, 540, 810and 1080 degrees

ω: the angular velocity of the eccentric shaft= 314.12 rad/sec

$$F_r = \frac{0.005}{9.81} 314.12^2 \left(\frac{0.077}{9} + 0.0109 cos \frac{2}{3} 0\right)$$

$$F_r = 0.9784 \text{ N}$$

The minimum inertia force at F_{rmin} is calculated by

$$F_{rmin} = \frac{W}{g} \omega^2 \left(\frac{R}{9} - e\right) \tag{1.5}$$

$$F_{rmin} = -0.1178\ N$$

Therefore, the force acting on the apex seal is converted to pressure.

$$P = \frac{F}{A} \tag{1.6}$$

$$P = 0.0119\ N\ /\ mm^2$$

Where, *F*- force acting on the apex seal

A-area of force acting

P- Pressure acting on apex seal

2.9. Kinematic analysis of Wankel engine

The motion study is conducted with the designed Wankel rotary engine to check the performances of the engine. The important values like the stiffness of spring, and forces acting on apex are calculated. Motion study includes (housing, rotor, eccentric shaft, apex seal and phasing gear), the calculated stiffness values are given between the rotor corner and bottom of the apex seal, the shaft is assigned to a motor with speed 3000 rpm, the solid body contact set is given for three apexes faces and housing. The study is calculated for the given speed and forces. The below figure shows the performed motion study and results of the motion study.

Spring stiffness calculations

$$K = \frac{8Ebt^3}{3L^3} \tag{2.18}$$

Where 65Mn spring material is used as a spring in the rotary engine I am using 65Mn material properties to calculate stiffness.

E- young's modulus=$200 * 10^9\ N\ /\ m^2$

b- width of spring = 0.002 m

L- length of spring = 0.048 m

t- thickness of spring = 0.001 m

$$K = \frac{8 * 200 * 10^9 * 0.002 * 0.001^3}{3 * 0.048^3}$$

$$K = 9645.06\ N/m \approx 9.645\ N/mm$$

Boundary condition

spring stiffness K – 9.645 N/mm

speed of the shaft N- 3000 rpm

contact between apex seal and housing

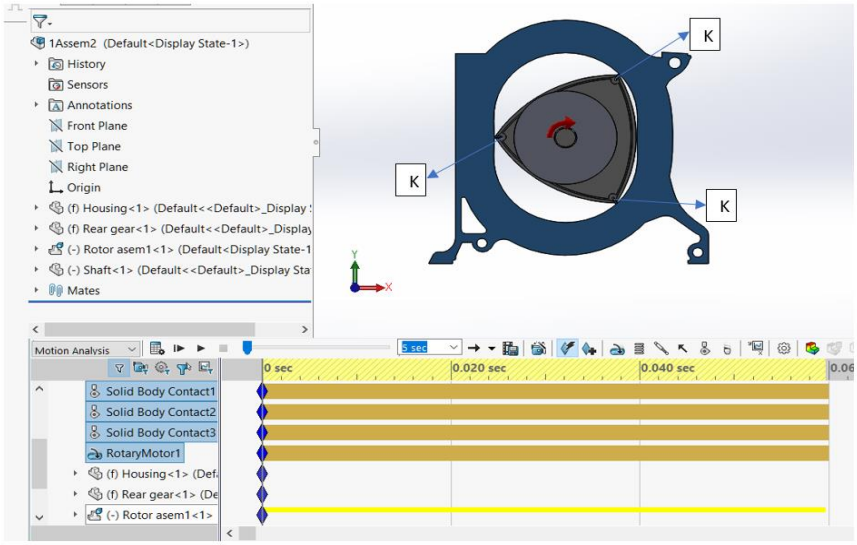

Fig 2.8- Kinematic study (using Solidworks 2016)

By using the formula velocity of rotor vertex is calculated. The calculated values and the simulated values of a Wankel engine are compared. This comparison is made to see the simulated and theoretical values meet the same results. The boundary condition specifies the input to conduct the motion study.

Calculation of the velocity of rotor vertex.

The circumferential velocity of the rotor apex is one representative value denoting the sliding velocity of the rotating components, which also defines the characteristics of the engine, along the trochoid constant.

$$v = \frac{\omega}{3}\left(9e^2 + R^2 + 6eR\cos {}^{2}/_{3}\,\alpha\right)^{1/2} \tag{1.1}$$

Where *e*- eccentricity of rotor = 10.9 mm

R- eccentricity radius of rotor = 80 mm

ω- angular velocity of rotating shaft = 314 rad/sec

α-shaft rotating angle =0,270,540,810,1080 degree

$$\text{At } \alpha = 0, \quad v = \frac{314}{3}\left(9 * 10.9^2 + 80^2 + 6 * 10.9 * 80 * cos\, {}^{2}/_{3}\, 0\right)^{1/2}$$

$$v = 11800.817\ mm/sec$$

$$At\ \alpha = 270, \quad v = \frac{314}{3}\left(9 * 10.9^2 + 80^2 + 6 * 10.9 * 80 * cos\, {}^{2}/_{3}\, 270\right)^{1/2}$$

$$v = 4952.78\ mm/sec$$

The calculated values of the velocity of rotor vertex are compared with the simulated values of the Solidworks motion study and below figure shows the comparison graph.

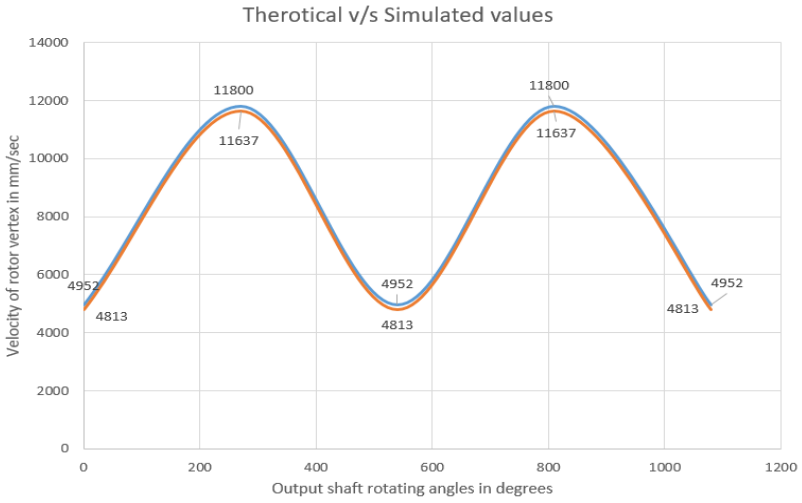

Fig 2.9- Comparison of theoretical and simulated velocities.

The blue line shows the calculated values by using formula and the orange line is the result obtained in the Solidworks motion study. The calculated values are more than simulated values, but the theoretical values are nearer to the calculated values. The above fig 2.9 shows the plot of calculated and simulated values the theoretical values are nearer to the calculated values, hence, the designed model meets the required values.

Contact forces between housing and rotor apex

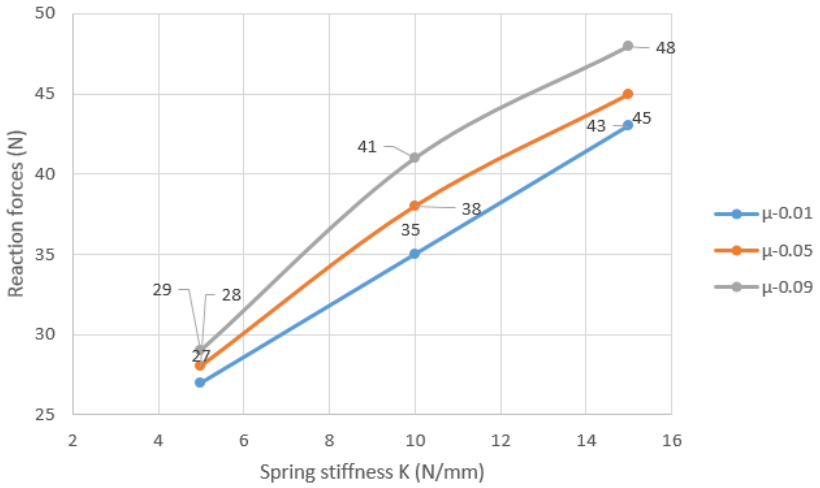

Fig 2.10- Reaction forces at different spring stiffness K

The above fig 2.10 shows the plot of reaction forces between apex seal and rotor housing. The motion study is conducted for different spring stiffness 5, 10 and 15 N/mm with different coefficients of friction (μ=0.01, 0.05 and 0.09) to check the reaction forces between apex seal and rotor housing. The obtained reaction forces result in different stiffness are 27, 35 and 45 newtons at μ=0.01, by increasing the stiffness of the spring the reaction forces between the apex seal and rotor housing also increases. So, we can say that by increasing the stiffness value K we can achieve proper sealing and reduce leakage between the apex seal and rotor housing. By using lubricants, the reaction forces will reduce little, but not too much. The above graph shows the reduction of reaction forces while reducing the coefficient of friction.

Frictional forces between housing and rotor apex

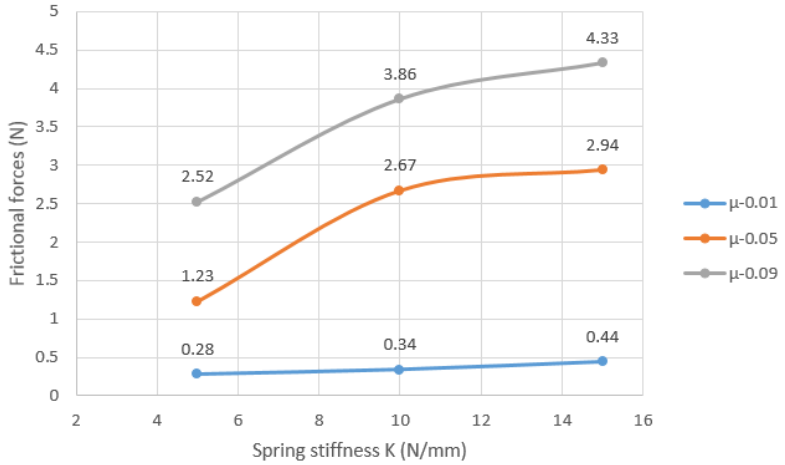

Fig 2.11- Frictional forces at different spring stiffness K

The fig 2.11 shows the plot of frictional forces between housing and apex seal. The motion study is conducted for different spring stiffness 5, 10 and 15 N/mm with different coefficients of friction (μ=0.01, 0.05 and 0.09) to check the frictional forces between apex seal and rotor housing. As known that if spring stiffness increases the friction force also increases. To reduce the frictional force, the apex seal surface is made smoother or coated with lubricated materials. From the above 2.11 graph, we can see that by reducing the coefficient of friction the frictional force will be reduced.

3. COMPUTATIONAL FLUID DYNAMICS ANALYSIS

The objective of CFD is to find the forces acting on the rotor. CFD is conducted on the whole Wankel engine to find force acting on the Wankel rotor due to pressure 120 bar at power stroke. In this study, fluent medium used is AFR (Air fuel mixture) of diesel. The boundary conditions are inlet pressure 1 bar, exhaust 0.5 bar and 120 bar at ignition. The results are exported for FEA as loads. The forces acting on apex seal are calculated before conducting CFD. The forces like (spring force and resultant forces) are calculated in chapter-2 and used in CFD.

3.1. Fluid Analysis and Discussion

The Navier-Strokes Equation for Laminar and Turbulent Fluid Flow

The Navier-Stroke equation is used to solve the flow simulation, that includes formulation of mass, and energy conversion laws for fluid flows. The equations are used by the fluid state equation signifies the nature of the fluid, and empirical needs of fluid density, viscosity and thermal conductivity with temperature. A problem is finally detailed by the definition of its geometry, boundary and initial conditions. Turbulent and laminar flows can be predicted by flow simulation. When the Reynolds number is small we can see laminar flow. When the Reynolds number increases to critical value, the flow turn into turbulent [33].

Turbulent is considered for the most of engineering practice fluid flows, so simulation mainly considered for study and simulate turbulent flows. The Favre-averaged Navier-Stokes equations are used to predict turbulent flow, time-averaged effects of the flow turbulence on the flow parameters are taken into account, i.e. large-scale, time-dependent phenomena are considered directly. Flow Simulation uses k-ϵ equations for the turbulent kinetic energy and its dissipation rate, the so is known as k-ϵ model [33].

$$\frac{\partial \rho}{\partial t} + \frac{\partial}{\partial x_i}(\rho u_i) = 0, \tag{3.1}$$

$$\frac{\partial \rho u_i}{\partial t} + \frac{\partial}{\partial x_j}\left(\rho u_i u_j\right) + \frac{\partial p}{\partial x_i} = \frac{\partial}{\partial x_j}\left(\tau_{ij} + \tau_{ij}^R\right) + S_i = 1{,}2{,}3\tau \tag{3.2}$$

$$\frac{\partial \rho H}{\partial t} + \frac{\partial \rho u_i H}{\partial x_i} = \frac{\partial}{\partial x_i}\left(u_j\left(\tau_{ij} + \tau_{ij}^R\right) + q_i\right) + \frac{\partial p}{\partial t} - \tau_{ij}^R \frac{\partial u_i}{\partial x_j} + \partial + S_i u_i + Q_H, \tag{3.3}$$

$$H = h + \frac{u^2}{2}$$

3.1.1. Governing Equations

The Solidworks CFD (Computational fluid dynamics) is used in this study. The k-ϵ model energy equation is used in Computational Fluid Dynamics (CFD) to simulate mean flow characteristics for turbulent flow conditions. The k-ϵ model is the two-equation model which gives a description of turbulence by using the two transport equations: [33]

These are the equations,

$$\frac{\partial \rho k}{\partial t} + \frac{\partial}{\partial x_i}(\rho u_i k) = \frac{\partial}{\partial x_i}\left(\left(\mu + \frac{\mu_t}{\sigma_k}\right)\frac{\partial k}{\partial x_i}\right) + S_{k,} \tag{3.4}$$

$$\frac{\partial \rho \epsilon}{\partial t} + \frac{\partial}{\partial x_i}(\rho u_i \epsilon) = \frac{\partial}{\partial x_i}\left(\left(\mu + \frac{\mu_t}{\sigma_\epsilon}\right)\frac{\partial \epsilon}{\partial x_i}\right) + S_{\epsilon,} \tag{3.5}$$

Where the source terms $S_k \; and \; S_\epsilon$are defined as

$$S_k = \tau_{ij}^R \frac{\partial u_i}{\partial x_j} - \rho\epsilon + \mu_t P_B \tag{3.6}$$

$$S_k = C_{\epsilon 1}\frac{\epsilon}{k}\left(f_1 \tau_{ij}^R \frac{\partial u_i}{\partial x_j} + \mu_t C_B P_B\right) - C_{\epsilon 2} f_2 \frac{\rho \epsilon^2}{k} \tag{3.7}$$

Here P_B represents the turbulent generation due to buoyancy forces,

$$P_B = -\frac{g_i}{\sigma_B}\frac{1}{\rho}\frac{\partial \rho}{\partial x_i} \tag{3.8}$$

$$f_1 = 1 + \left(\frac{0.05}{f_\mu}\right)^3, f_2 = 1 - \exp(-R_T^2) \tag{3.9}$$

The constants $C_\mu, C_{\epsilon 1}, C_{\epsilon 2}, \sigma_k, \sigma_\epsilon$ are defined empirically. [34]

3.1.2. Assumption and Boundary Conditions

Input conditions are as follows:

- The fluid is analysed using a turbulence model (k-ϵ model)
- inlet pressure- 1 bar
- exhaust pressure- 0.5 bar
- pressure at power stroke- 120 bar [34]
- forces acting on apex seal - 0.119 bar

- air fuel mixture density of diesel- 1.38 kg/m^3 [35]
- conjugate heat transfer and radiation effects are neglected.

By using the above input conditions the fluid analysis is computed, during operation, the effect of the gas pressure acts on the rotor face. To get proper impact the tiny clearance between rotor and housing is provided. The computed analysis results are used to do the static linear study to know the stresses acting on the rotor and fatigue study are conducted to check the life of the rotor at the above-given 120 bar pressure.

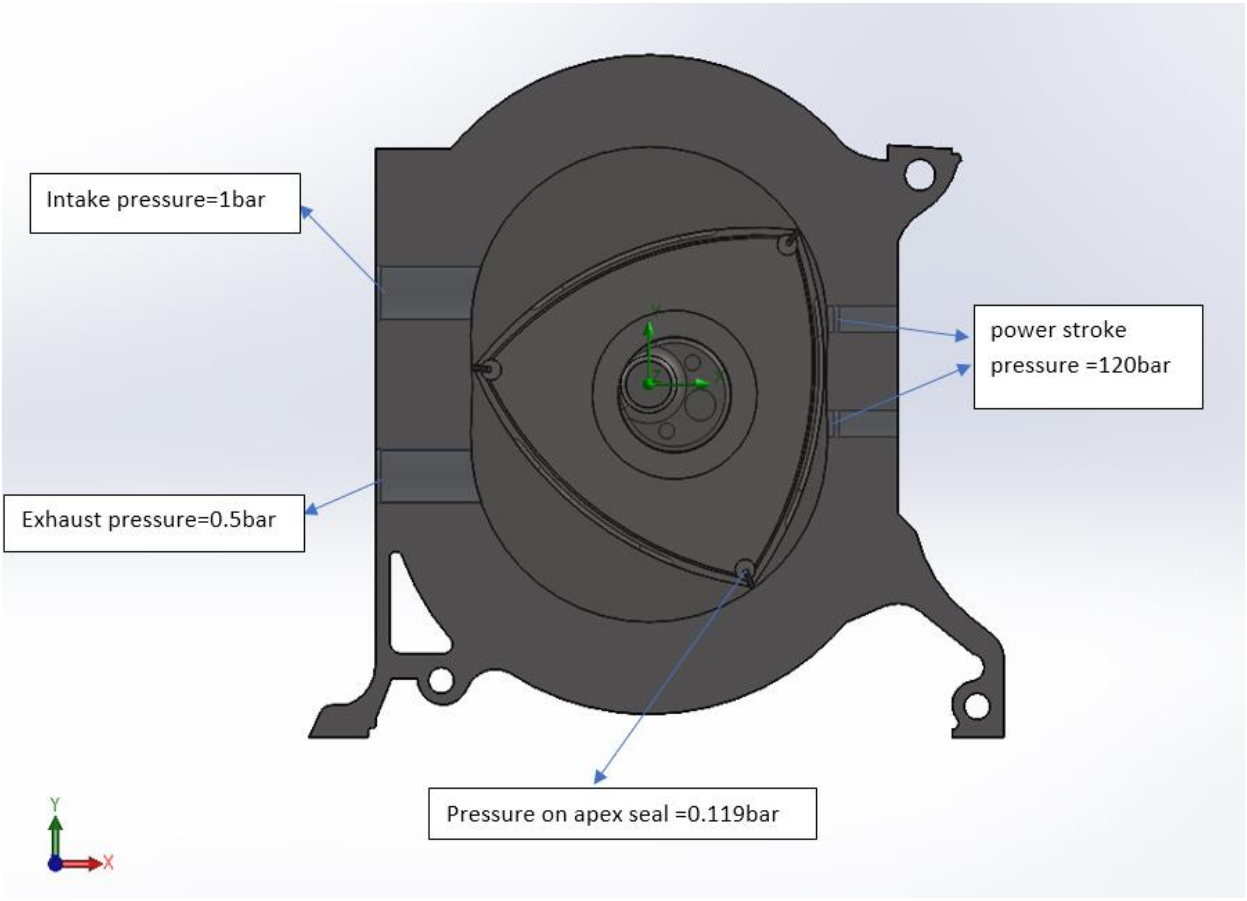

Fig 3.1- Computational Fluid Analysis.

The fig 3.1 shows the model of the Wankel engine with all the boundary conditions. The CFD is computed to the wankel engine by considering all the above given boundary conditions. The results obtained are tabulated.

Table 3.1- Pressure results obtained from goal plots

Name	Minimum value (Pa)	Maximum value (Pa)
Static pressure	1.22e+007	1.25e+007
Total pressure	1.90e+007	1.91e+007
Dynamic pressure	1.95e+007	1.95e+007

The table 3.1 shows the minimum and maximum pressures. The results from the CFD is Exported to static study to see the forces acting on the rotor and apex seal.

4. STATIC AND FATIGUE ANALYSIS

The results from CFD is directly imported as forces acting on the rotor, apex seal and the static study is conducted.

The objective of FEA is to study the stresses and displacement of the rotor. The stresses obtained can be used to predict the fatigue life and determine the failure regions. The linear elastic study was used since the rotor is designed for longer life. In the study, the rotor centre is fixed and the loading conditions is imported from the CFD study. And further proceeding to fatigue with loading ratio R=0 (unidirectional stress) to calculate the exact life of the rotor. This fatigue study is calculated for two materials and the results of fatigue life are compared. Since

$$R = \frac{\sigma_{min}}{\sigma_{max}} \tag{1.12}$$

Table 4.1- Material properties of Ductile cast iron and Aluminium 7075-T6 [37]

Mechanical properties v/s Material	**Ductile cast iron**	**Aluminum 7075-T6**
Elastic Modulus	120000 MPa	72000 MPa
Poisson's ratio	0.31	0.33
Shear modulus	77000 MPa	26900 MPa
Mass Density	7100 Kg/m^3	2810 Kg/m^3
Tensile strength	861.695 MPa	570 MPa
Yield strength	551.485 MPa	505 MPa
Specific heat	450 J/(kg-K)	960 J/(kg-K)

The table 4.1 shows the material properties of ductile cast iron and aluminium 7075-T6 and below fig 4.1 shows the S-N curves of both the materials.

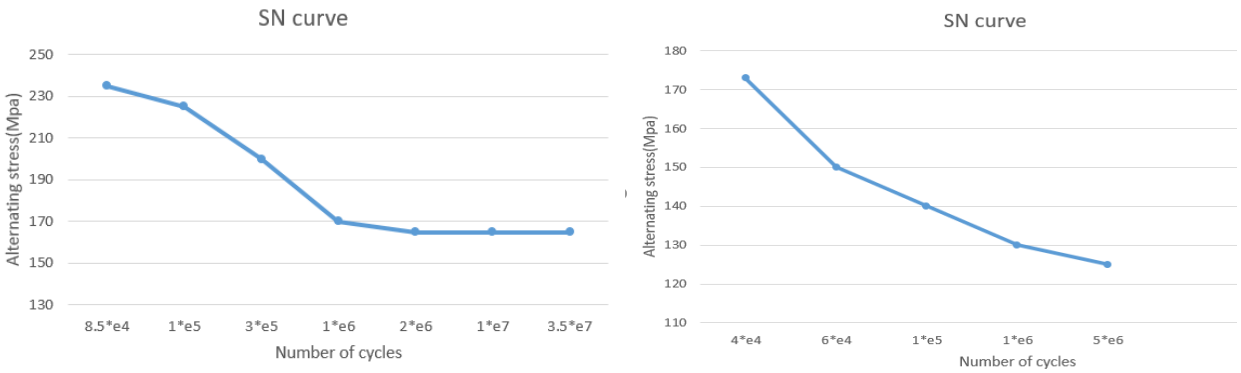

Fig 4.1- S-N curve for Ductile Cast iron and Aluminium 7075-T6 (Solidworks 2016)

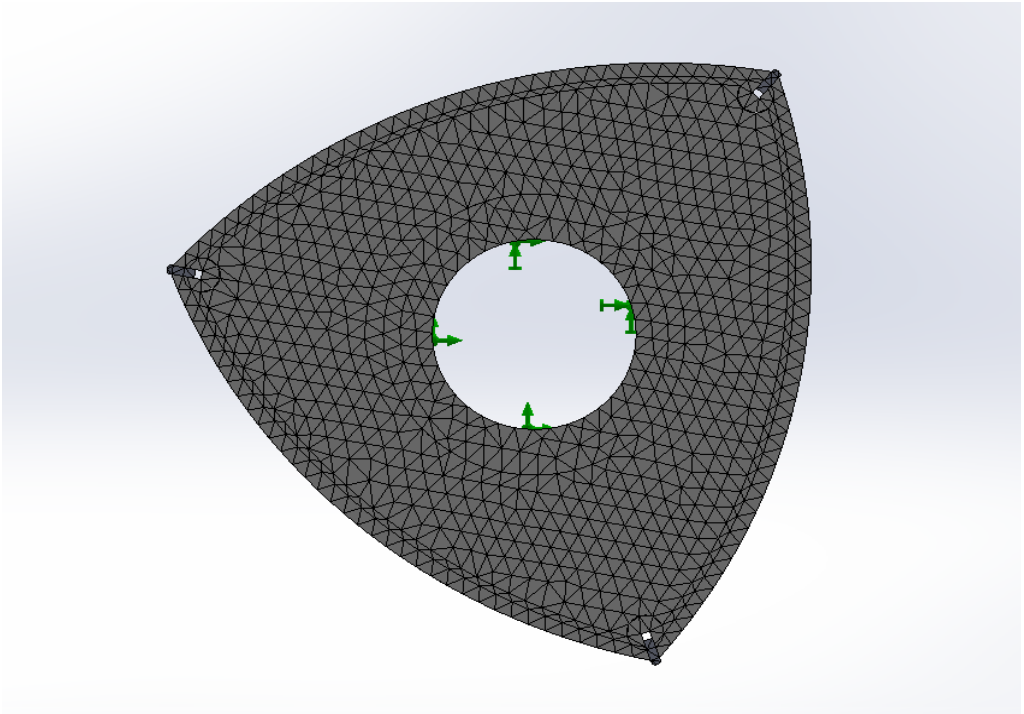

Fig 4.2- Rotor mesh

The static study is considered for the rotor with apex and all the design parameters of a rotor are explained in chapter-2. The above figure 4.2 shows the meshed model of a rotor and the centre of the rotor is fixed by assuming that the forces from CFD are acting on one surface of the rotor face due to power stroke. Standard mesh is used as mesher, mesh type is solid mesh, Jacobian 4points, element size 4mm, tolerance 0.2mm, total nodes 100066 and total elements 67686 are used in the study.

The R-ratio is considered as unidirectional then R=0, the force acting on the rotor face is a compressive force there is no tensional force hence it is considered as unidirectional. The R-ratio will be 0 therefore, the minimum stress will become zero. The von mises stress obtained from the static study is

considered to be maximum stresses acting on the rotor. The zoomed area of the figure shows the maximum stresses acting near the corner seal areas of corner.

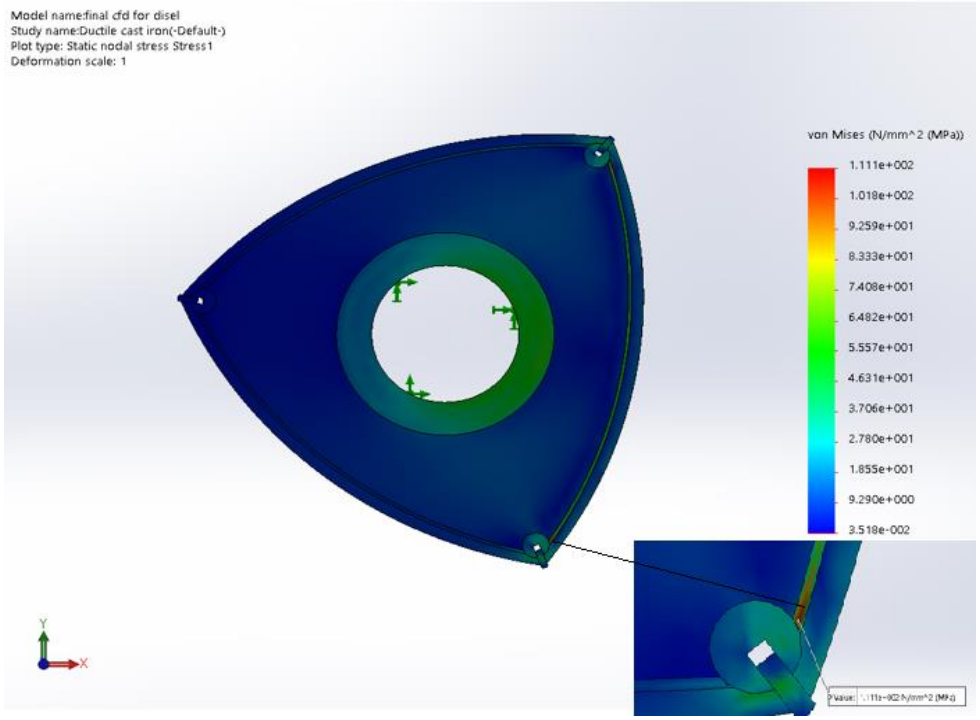

Fig 4.3- Von-mises stress for Ductile cast iron.

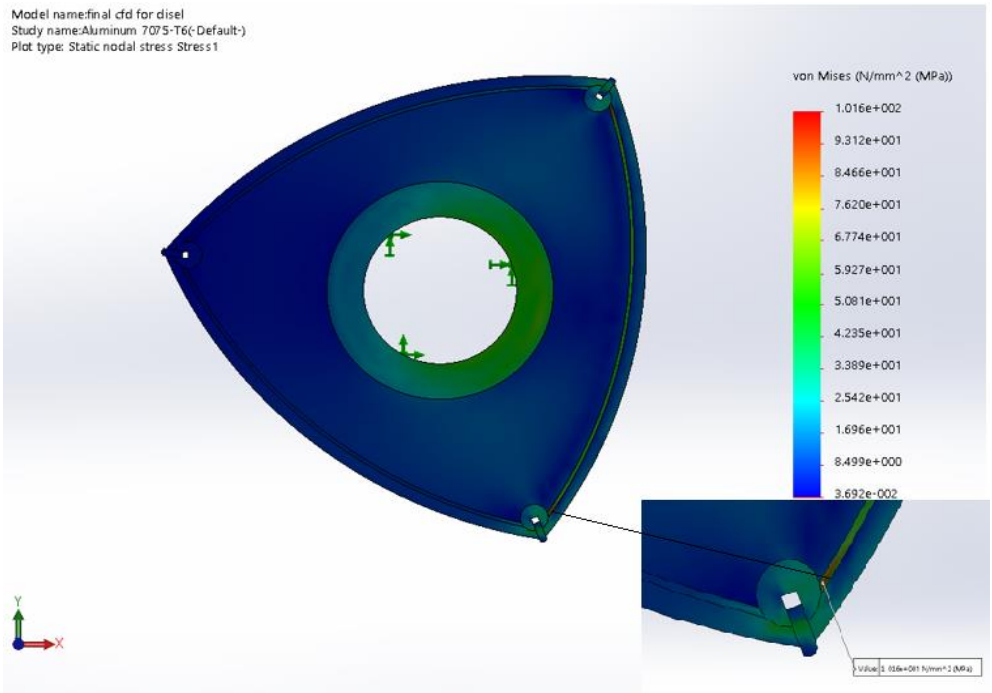

Fig 4.4- Von-mises stress for Aluminium 7075-T6

4.1. Calculation for fatigue life of rotor ductile cast iron for R=0 (forces from CFD)

From static study

Maximum von mises stress in compression loading

$$\sigma_{max} = 111.1\ MPa$$

Loading ratio R=0

$$\frac{\sigma_{min}}{\sigma_{max}} = 0$$

$$\sigma_{min} = 0$$

Mean stress

$$\sigma_{mean} = \sigma_m = \frac{\sigma_{max}+\sigma_{min}}{2}, \tag{1.11}$$

$$\sigma_m = 55.5\ MPa$$

Alternative stress

$$\sigma_{alternative} = \sigma_a = \frac{\sigma_{max}-\sigma_{min}}{2}, \tag{1.12}$$

$$\sigma_a = 55.5\ MPa$$

Factor of safety

$$FOS = \frac{yield\ stress}{Working\ stress}, \tag{4.1}$$

$$FOS = 5$$

To find Endurance strength S_e

$$S_e = S'_e * k_a * k_r * k_{sz} * k_{sr}, \tag{1.15}$$

$$S'_e = 0.4S_{ut}\ for\ S_{ut} < 400\ Mpa = 160MPa\ (cast\ iron)\ for\ all\ other\ value\ of\ S_{ut}$$

$$S_{ut} = 861.69\ MPa$$

$$S'_e = 160\ MPa$$

k_a −load correction factor for torsional load=1

$k_{reliability}$ −reliability-90%=0.92

$k_{sz} - size\ factor = 1$

$k_{sr} - surface\ finish\ factor = 1.2$

$$S_e = 160 * 1 * 0.92 * 1.2$$

$$S_e = 176.64\ MPa$$

To find the number of cycles from S-N construction

$$S_f = \frac{\sigma_a * S_{ut}}{S_{ut} - \sigma_m}, \tag{1.13}$$

$$S_f = 59.32\ MPa$$

$$0.9S_{ut} = 775.52\ Mpa$$

$\log_{10}(0.9S_{ut}) = 2.889$

$\log_{10}(S_e) = 2.248$

$\log_{10}(S_f) = 1.773$

$$\log_{10}(N) = \frac{(6-3)(\log_{10}(0.9S_{ut})) - \log_{10}(S_f)}{\log_{10}(0.9S_{ut}) - \log_{10}(S_e)} + 3 \tag{1.14}$$

$$N = 1.6714328 * 10^8\ cycles$$

4.2. Calculation for fatigue life of rotor aluminium 7075-T6 (forces from CFD)

From static study

Maximum von mises stress in compression loading

$$\sigma_{max} = 101.6\ MPa$$

Loading ratio R=0

$$\frac{\sigma_{min}}{\sigma_{max}} = 0$$

$$\sigma_{min} = 0$$

Mean stress

$$\sigma_{mean} = \sigma_m = \frac{\sigma_{max} + \sigma_{min}}{2}, \tag{1.10}$$

$$\sigma_m = 50.8\ MPa$$

Alternative stress

$$\sigma_{alternative} = \sigma_a = \frac{\sigma_{max} - \sigma_{min}}{2}, \quad (1.11)$$

$$\sigma_a = 50.8\ MPa$$

Factor of safety

$$FOS = \frac{yield\ stress}{Working\ stress}, \quad (4.2)$$

$$FOS = 4.96$$

To find Endurance strength S_e

$$S_e = S'_e * k_a * k_r * k_{sz}, k_{sr}, \quad (1.15)$$

$$S'_e = 0.4S_{ut}\ for\ S_{ut} < 400MPa = 130MPa\ (aluminium\ ) for\ all\ other\ values\ of\ S_{ut}$$

$$S_{ut} = 570\ MPa$$

$$S'_e = 130\ MPa$$

k_a −load correction factor =1

$k_{reliability}$ −reliability-90%=0.92

$k_{sz} - size\ factor = 1$

$k_{sr} - surface\ finish\ factor = 1.2$

$$S_e = 130 * 1 * 1 * 0.92 * 1.2$$

$$S_e = 143.52\ MPa$$

To find the number of cycles from S-N construction

$$S_f = \frac{\sigma_a * S_{ut}}{S_{ut} - \sigma_m}, \quad (1.13)$$

$$S_f = 55.77\ MPa$$

$$0.9S_{ut} = 513\ Mpa$$

$\log_{10}(0.9S_{ut}) = 2.710$

$\log_{10}(S_e) = 2.156$

$\log_{10}(S_f) = 1.786$

$$\log_{10}(N) = \frac{(6-3)(\log_{10}(0.9S_{ut}))-\log_{10}(S_f)}{\log_{10}(0.9S_{ut})-\log_{10}(S_e)} + 3 \quad (1.14)$$

$$N = 1.0083472 * 10^8\ cycles$$

Table 4.2- Calculated results.

S.no.	Materials	Loading ratio R	Mean stress $\sigma_m\ (MPa)$	Alternating force $\sigma_a\ (MPa)$	$f.o.s$	Number of cycles N_f
1	Ductile cast iron	0	55.5	55.5	5	$1.6714328 * 10^8\ cycles$
2	Aluminum 7075-T6	0	50.8	50.8	4.96	$1.0083472 * 10^8\ cycles$

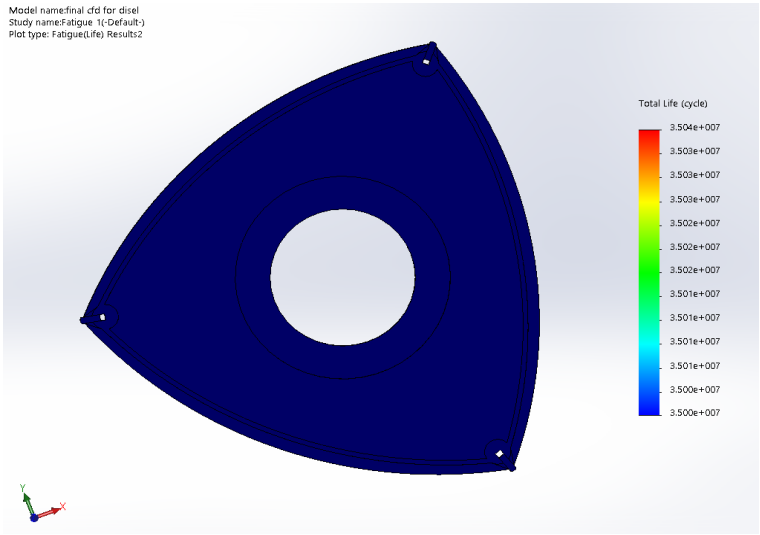

Fig 4.5- Fatigue study showing infinity life

The fig 4.3 and 4.4 shows the maximum stress absorption is at the corner of the corner seal. The table 4.2 shows the mean and alternative stress in different materials and the fatigue life cycles are tabulated. The Ductile cast iron responded with better life cycle than the aluminium. The fig 4.5 shows the infinite fatigue life obtained in the Solidworks fatigue analysis. The fatigue analysis for both materials shows the stresses acting on the rotor are below the endurance stress since there is no crack initiation below $3.5 * 10^7$. As it is said a component beyond $1 * 10^6$ cycles will have infinity life.

5. K-FACTOR EFFECT ON WANKEL ENGINE

The ratio of the radius *R* with respect to the eccentricity *e* is known as trochoid constant *K*, the constant K will provide a profile curve by using radius and eccentricity.

$$K=R/e \tag{5.1}$$

The Wankel engine is a rotary engine it uses a rotor instead of a piston, the pressure acting on rotary is converted into rotating motion by using eccentric shaft. The Wankel engine consists of two main parts in the engine that is housing chamber and rotor. The 3 tips of rotor divide the housing into 3 chambers. The relevant research on rotary engine provides the different theory for creating an outline of the casing, but this particular research focuses on Peritrochoid theory as discussed in chapter-2. There are several problems remained to be solved, working chamber and sealing of a rotor.

The important parameter to be considered for the engine performance is a geometrical design of rotary profile. The work on K-factor provides the study flow features of different geometric design of the rotary profile by creating a fluid analysis model of a rotary engine. The three profiles of the rotary engine are designed by using the chapter-2 calculations and formulas.

Below table 5.1 shows the three profiles of the Wankel engine at different K-factor. By using the tabulated values the rotor profiles are designed. The length of the housing remains same but due to K-factor the profile curve of the rotor and housing changes.

Table 5.1- Geometrical parameters of different K-factor

Case/ K-factor	Eccentricity *e* (mm)	Length-*R* (mm)	K=*R/e*
Case-1	8.4	84.3	10
Case-2	10.9	81.8	7.5
Case-3	13.25	79.5	6

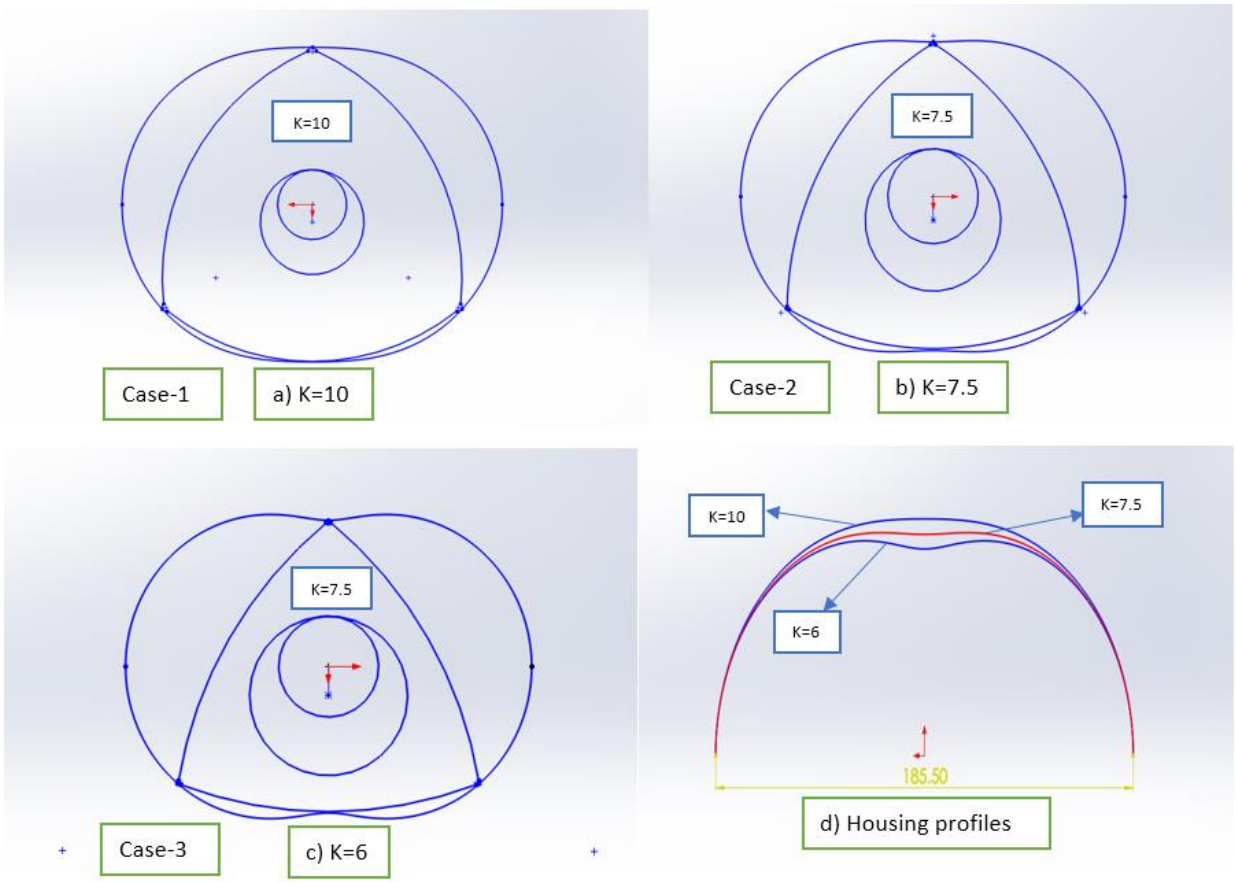

Fig 5.1- Rotary profiles of three cases.

5.1. Velocity plot for three cases with angle and clearance

Assumptions and boundary conditions

- Air is used as a fluid in this study (density of air-1.293 Kg/m^3 and viscosity-1.81E-05 Kg/m-s)
- the fluid is analysed using a turbulence model (k-ϵ model)
- inlet pressure is 2 bar
- outlet pressure is 1 bar
- Solidworks CFD with 3D geometry

During CFD study, the force acting on the rotor will try to move the rotor, a tiny clearance 0.1mm is provided between the apex seal and the housing, the results are compared with different profile and different cases.

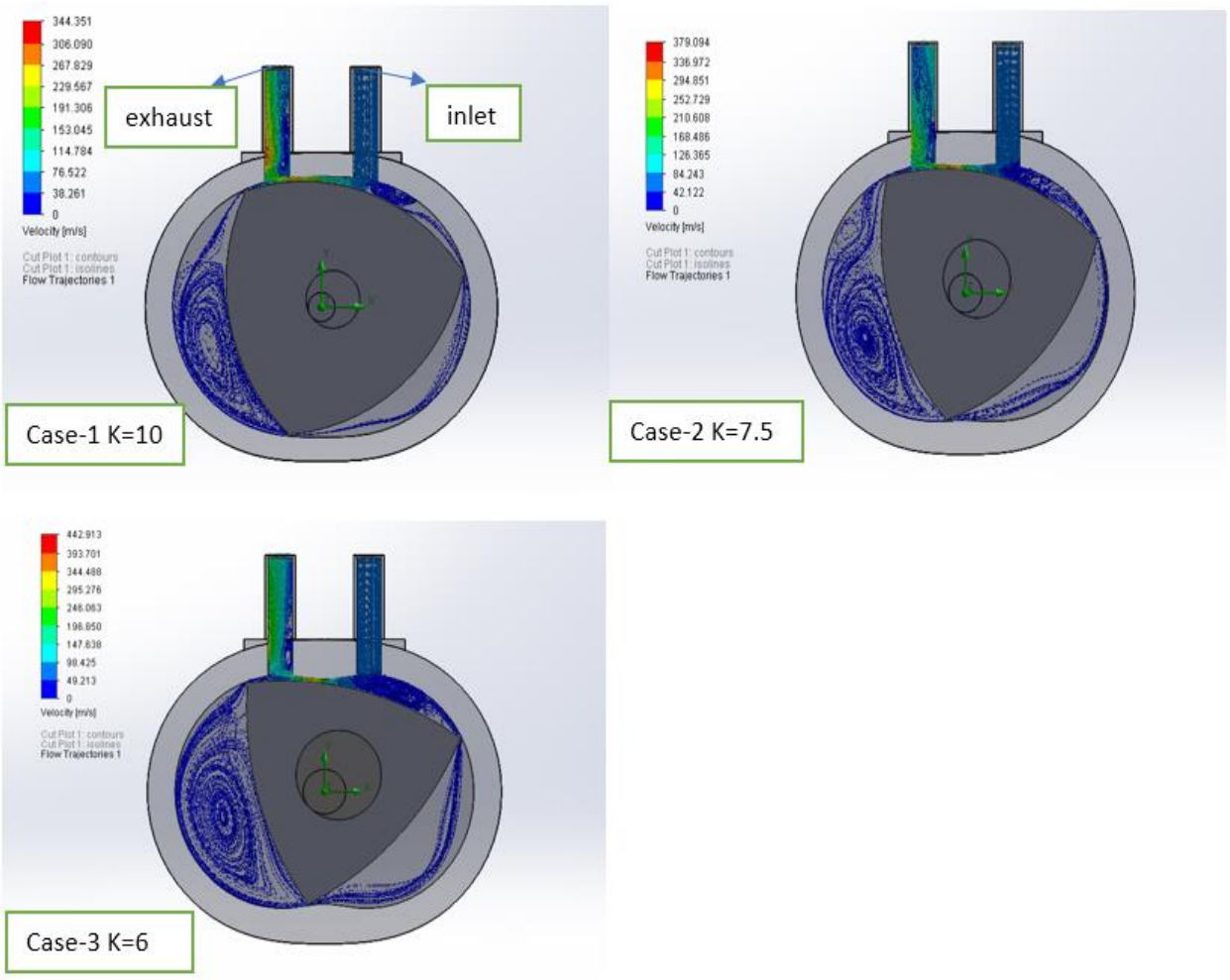

Fig 5.2- Velocity plot for three cases with rotation angle and clearance.

In fig-5.2, we can see the profiles of three rotary housings with different K-factor. Assuming the above condition for all the three profiles are maintained to the same pressure with the same clearance to get the proper results, the angle of the rotor is given as 20 degrees and conducted CFD in Solidworks to see the flow and leakage in between the rotor and housing. Now we can see the leakage in the three profiles, in case-1, the velocity of flow is 344.35 m/s, in case-2 the velocity of flow is 379.09 m/s and in case-3 the velocity of flow is 442.91 m/s. By comparing all the three results the maximum velocity of flow in case-3 we can say that the maximum leakage takes place in case-3 compared to other two cases the minimum velocity of flow in case-1 so that the leakage is minimum in case-1 compared to other two cases.

5.2. Leakage plots for three cases with 0.10mm clearance

In this study boundary condition is same as above mentioned the inlet will be 2 bar, outlet pressure 1 bar with the 0-degree angle of rotation geometry and maintaining 0.1mm clearance to see the flow, CFD is computed in Ansys fluent with 2D geometry. The below fig 5.3 shows the fine mesh of the profile of case-3 and the three profiles has meshed with an element size of 0.005. The table shows the 3 cases, mesh parameters and we can see that the case-3 has a more number of elements and nodes compared to other two cases so that working chamber will be more compared to other two cases.

Table 5.2- Meshed parameters of three cases.

Case	k-factor	Element size	Nodes	Elements	Velocity m/s
Case-1	10	0.0005	35426	34326	128
Case-2	7.5	0.0005	44779	43695	171
Case-3	6	0.0005	53546	52467	243

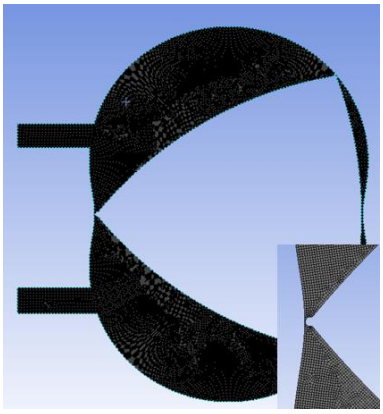

Fig 5.3- Meshed profile.

The fig 5.4 shows the velocity of flow, the more leakage we can see in case-3 due to more chamber space and the k-factor influence on the rotor profile. The flow of velocity proves that there is less leakage in case-1 compared to other two cases. The maximum velocity of flow is 243 m/s in case-3 and more impact flow of red we can see in the zoomed apex area. In all the 3-cases, there is more leakage in case-3. This observation indicates that an increase in internal pressure leads to more leakage. The analysis that clearly proves that design profile affects leakage and have the highest effect on the engine.

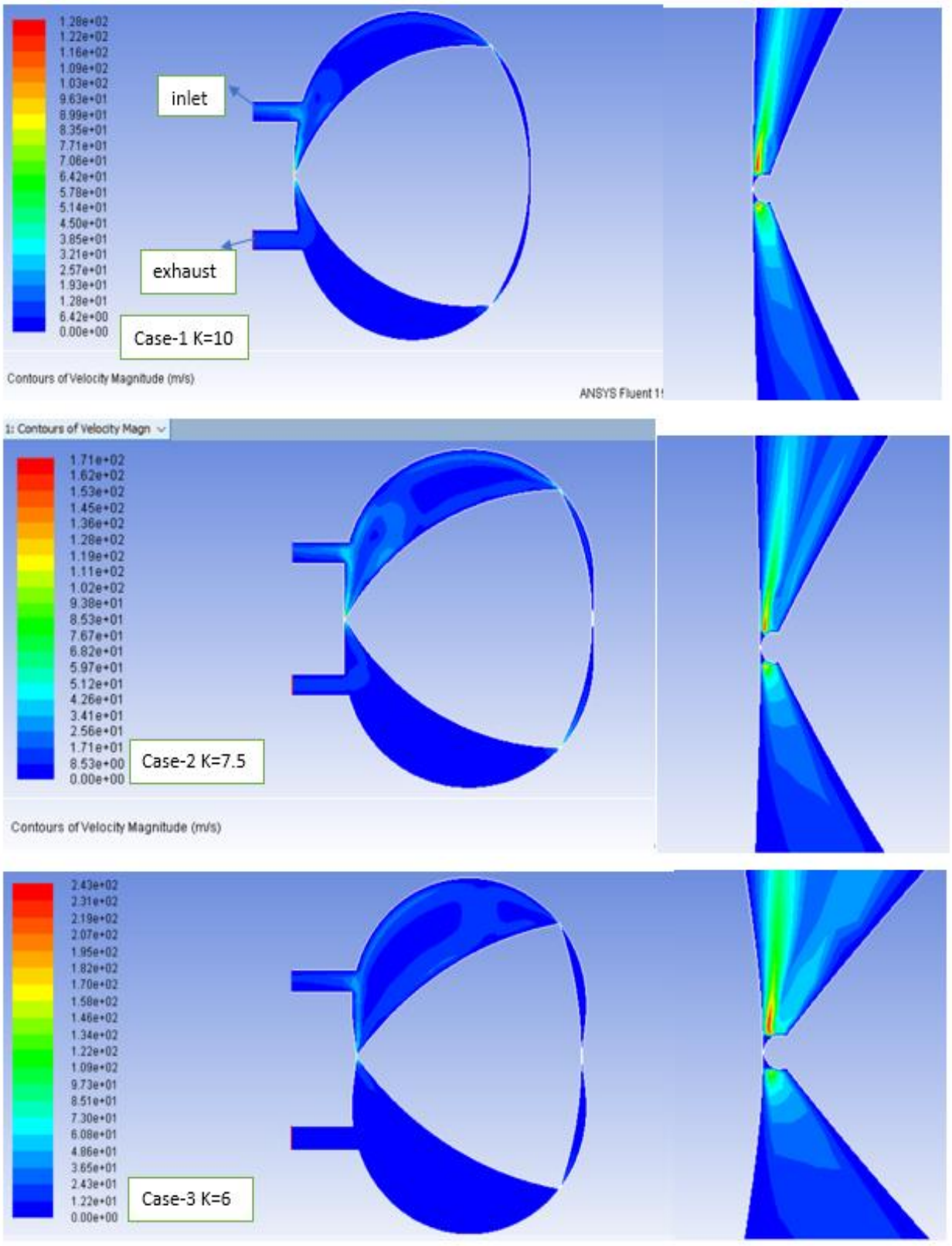

Fig 5.4- leakage plots for three cases with 0.10mm clearance.

5.3. Velocity plots for 3-cases without clearances

The fig 5.5 shows the three cases of rotary profile with 0 clearance at apex and housing. The picture in case-3 has a more velocity of flow 891 m/sec due to more chamber space and in case-2 we can see the velocity of flow is 741 m/sec and 525 m/sec at case-1. So, that the lesser k-factor has a more working chamber and higher k-factor has less working chamber.

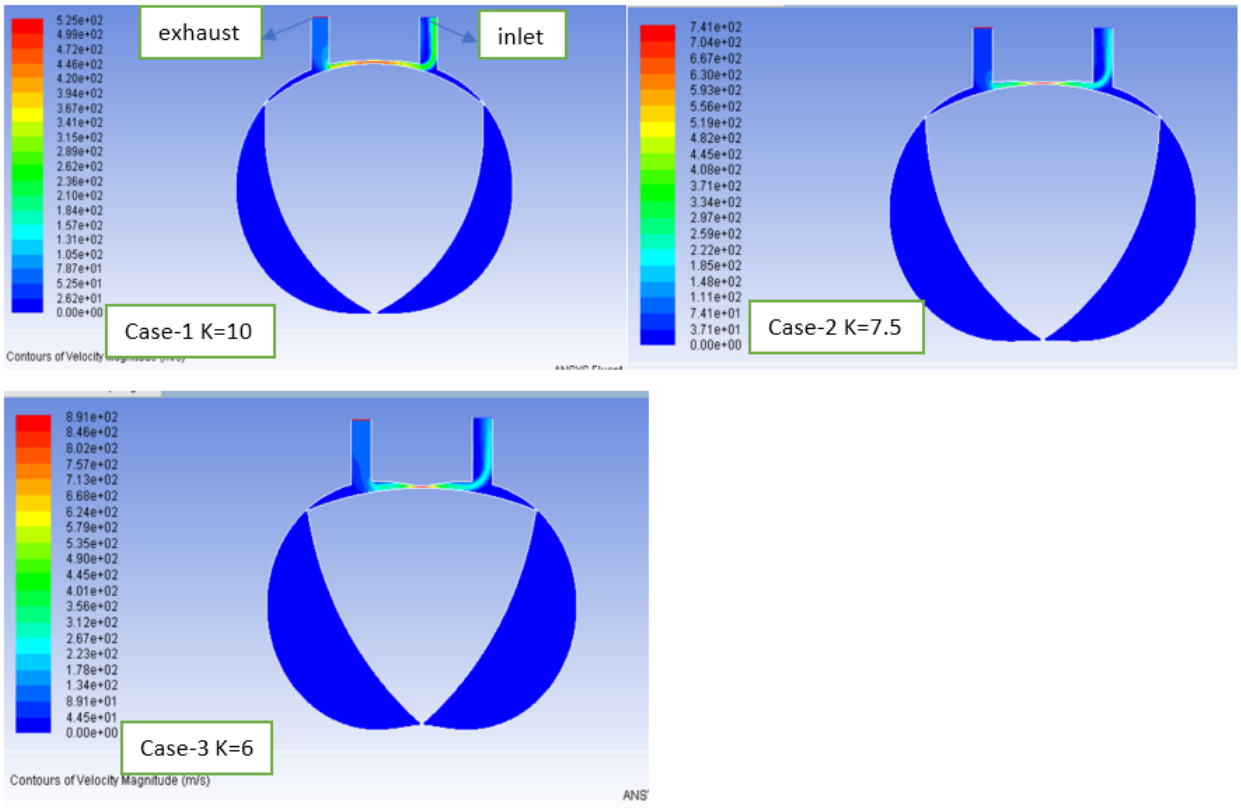

Fig 5.5- Velocity plot for three profiles without clearance.

Conclusion

- The conclusion that could be drawn from literature survey, the engine is to be designed is similar to the existing one (the engines like 13B and Rensis is considered to design a model) but the two-piece apex seal is replaced by a single piece improved new apex seal.
- The motion study is conducted by using Solidworks motion study. The velocity of rotor vertex is calculated theoretically and the results are compared with the simulated values. The results simulated are 11637 mm/sec and results from theoretical calculated values are 11800 mm/sec. Hence the maximum velocity, which is derived is more than stimulated but nearer to the initial calculated approximation. The contact force and friction forces are simulated for different spring stiffness K (5,10 and 15 N/mm) with different coefficients of friction (μ=0.01, 0.05 and 0.09). The results of reaction forces are 27, 35 and 45 N, the frictional forces are 0.28, 0.34 and 0.44 N. So, by increasing spring stiffness we can achieve better sealing and by reducing the coefficient of friction we can reduce frictional forces.
- The CFD study is conducted to investigate the flow characteristics and the resulting stress acting on the rotor at a 120-bar pressure on a power stroke. The maximum static pressure obtained in CFD is 1.25e+007 pascals, the results are further exported to static study.
- The obtained results from CFD are exported to static analysis to check the stress acting on the rotor. The static study is conducted for two materials, namely ductile cast iron and AL7075-T6 where the maximum stress acting on the rotor is 111 MPa and 101.6 MPa. The fatigue study is conducted to check the life of the rotor and compared with the life cycle predicted for the rotor for both material Ductile cast iron and Al 7075-T6. Hence table-3.2 shows that the Ductile cast iron with $1.67 * 10^8$ cycles and Al 7075-T6 has $1.008 * 10^8$ cycles. Based on the results, Ductile cast iron is much more reliable than Al 7075-T6 as providing longer life. By using Al 7075-T6 the weight of the engine is decreased from 16.1 to 14.08 Kg, the speed will be increased due to less mass of the material.
- The various geometries are designed with various K-factor and the figure-5.1 shows the different rotary profiles for different K-factor.
- To study the effects of different K-factor design profile on rotary engine flow characteristics, three different profile curves with different K-factor are designed and analysed using Ansys Fluent. The carried out 2D CFD analysis showed that case-3, has the maximum velocity of flow 243 m/sec, case-2 with 171 m/sec and case-1 with 128 m/sec. K-factor=6, have a higher working chamber with higher compression efficiency and while with K-factor=10 have less working

chamber and lower compression efficiency. Lower the K-factor with higher leakage, high internal pressure and high velocity of flow. Similarly, with a higher K-factor value, it leads to low leakage, small internal pressure and less velocity of flow. The above compared results of different K-factor influences that, while designing a rotary engine, designers must take k-factor into consideration. The research on the different profiles of K-factor serves useful information for the consideration of K-factor while engine designing.

- The created 3D model of the engine was animated by using Solidworks composer, rendering for appearance and the assembly drawings of Wankel engine were created with all necessary values by using Solidworks drawings.

REFERENCE

1. Alexandru Radu Chis: Wankel's Rotary, Internet document, April 2010 [accessed on May 2017]. https://www.autoevolution.com/news/how-wankels-rotary-engine-works-19241.html
2. The new world encyclopaedia [accessed on May 2017]. http://www.newworldencyclopedia.org/entry/Engine
3. The new world encyclopaedia internal combustion engine [accessed on May 2017].http://www.newworldencyclopedia.org/entry/Internal_combustion_engine#Wankel
4. The Museum of Retro Technology." Rotary Internal Combustion Engine". [accessed on May 2017]. http://www.douglas-self.com/MUSEUM/POWER/unusualICeng/rotaryIC/rotaryIC.htm
5. The Murdock's rotary steam engine patent: US2302 A of Oct 11, 1841 [accessed on May 2017]. https://www.google.com/patents/US2302
6. The Behren's rotary steam engine patent: US53915 A OF April 10, 1866 [accessed on May 2017]. https://www.google.com/patents/US53915
7. Kenichi Yamamoto, A text book of *Rotary Engine* in 1981. https://www.scribd.com/document/51077247/REbyKenichiYamamoto-1981
8. J. B. Umpleby (Petroleum Division A.I.M.E): December 1927 [accessed on May 2017]. https://doi.org/10.2118/927011-G
9. Maillard's rotary compressor patent: US4012180A of Mar 15, 1977 [accessed on May 2017]. https://www.google.com/patents/US4012180
10. Wankel engine patent: US5056315A Oct 15, 1991[accessed on May 2017]. https://www.google.com/patents/US5056315
11. Rotary engine: press information October,1999. [accessed on May 2017]. http://asmic.com/collect/rotary1999/rotary_e.pdf
12. Mazda Webpage: [accessed on May 2017]. http://www.mazdarotary.net/technical.htm
13. The Wankel motor, Internet document [accessed on May 2017]. http://der-wankelmotor.de./Felix_Wankel/felix_wankel.html
14. Johnsinit, The Wankel Engine – PART III – Problems and Disadvantages, November 2008, [accessed on May 2017]. http://www.brighthubengineering.com/machine-design/4948-the-wankel-engine-part-iii-problems-and-disadvantages/
15. Newspaper article on Apex seal [accessed on May 2017]. http://www.rotaryeng.net/history.html

16. Centenaro Stefano and Furlan Ismaele, Wankel engine kinematic study, Internet Article: [accessed on May 2017]. http://www.multibody.net/teaching/msms/students-projects-2014/wankel-engine/
17. De-Lou Zhang, Yu-ting Wu, Jing-Fu Wang, Chun-Xu Du, Xia Chen, Rui Ma, and Chong-fang Ma, Theoretical Study of Seal Spring in a Wankel Compressor: International Compressor Engineering Conference. Purdue University 2016,
18. Badr, O., Naik, S., O'Callaghan, P., & Probert, S. (1991). Rotary Wankel Engines as Expansion Devicese in Steam Rankine-Cycle Engine. Applied Energy, 59-76.
19. Leonid Tartakovsky, Vladimir Baibikov, Marcel Gutman and Mark Veinblat, SAE International, Simulation of Wankel engine, October 2012. doi:10.4271/2012-32-0098
20. Albert Boretti, Modelling unmanned aerial vehicle jet ignition wankel engines with CAE/CFD, Journal, April 2015. ISSN: 2287-5271 DOI:
21. ZHAO Yuqiao, Loh Wai Lam, and Lee Thong-See, CFD Simulation of a Pump with Wankel Engine Geometry, Asian International Conference, November 21-23, 2011, IIT Madras, Chennai, India
22. Baowei Fan, Jianfeng Pan, Wenming Yang, Hui An, Aikun Tang, Xia Shao & Hong Xue (2015) Effects of different parameters on the flow field of peripheral ported rotary engines, Engineering Applications of Computational Fluid Mechanics, 9:1, 445-457
23. Chol-Bum M. Kweon, A Review of Heavy-Fuelled Rotary Engine Combustion, Army Research Laboratory, May 2011. ISSN: ARL-TR-5546.
24. Deepan Marudachalam M. G, K. Kanthavel, R. Krishnaraj, Optimization of shaft design under fatigue loading using Goodman method, International Journal of Scientific & Engineering Research, Volume 2, Issue 8, August-2011.
25. R. A. Gujar, S. V. Bhaskar, Shaft Design under Fatigue Loading by Using Modified Goodman Method, International Journal of Engineering Research and Applications, Volume 3, Issue 4, July 2013. ISSN: 2248-9622.
26. C.C. Osgood; Fatigue Design, 2nd Edition.1982.
27. R.C. Juvinall; Engineering consideration of stress, strain and strength, 1967
28. Michael Irvin Resor, Computational Investigation of Rotary Engine Homogeneous Charge Compression Ignition Feasibility, Master thesis, Wright State University, 2012.

29. Chiu-Fan Hsieh & Hao-Yu Cheng, Effects of Various Geometric Designs on the Flow Characteristics of a Triangular Rotary Engine, Mechanical Engineering Research; Vol. 5, No. 1; 2015, ISSN 1927-0607.
30. Richard stone, A text book of Introduction to Internal Combustion Engine, Page8-10.
31. Internet document, [accessed on May 2017]. http://www.rotaryeng.net/
32. Kenichi Yamamoto, A text book of *Rotary Engine* in 1971.
33. Solidworks, Technical reference [accessed on May 2017]. https://d2t1xqejof9utc.cloudfront.net/files/18565/SW_CFD_technical_reference.pdf?1361897013
34. Internet document, Engineering forums [accessed on May 2017]. http://www.eng-tips.com/viewthread.cfm?qid=215499
35. Jeff Hartman, A text book of Nitrous Oxide Performance Handbook (2009)- page 37
36. Internet document, MakeltFrom.com: [accessed on May 2017]. http://www.makeitfrom.com/material-properties/Ductile-Nodular-Spheroidal-Cast-Iron

FORMAT	ZONE	NO.	DESIGNATION	NAME	QUANTITY	NOTES
			Documentation			
A2			PR-00.00.000 AD	Assembly drawing	2	A2
			Assembly Units			
A4		1	PR-00.01.000	Engine assembly	1	
A4		2	PR-00.02.000	Rotor assembly	1	
			Parts			
A4		3	PR-00.00.003	Rotor housing	1	
A4		4	PR-00.00.004	Rotor	1	
A4		5	PR-00.00.005	Ecentric shaft	1	
A4		6	PR-00.00.006	Back plate	1	
A4		7	PR-00.00.007	Front plate	1	
A4		8	PR-00.00.008	Phasing gear	1	
A4		9	PR-00.00.009	Apex seal	6	
A4		10	PR-00.00.0010	Apex spring	6	
A4		11	PR-00.00.0011	Corner seal	6	
A4		12	PR-00.00.0012	Corner cap	6	
A4		13	PR-00.00.0013	Rotor oil seal	1	
A4		14	PR-00.00.0014	Intake manifold	1	

Resp. department	Technical reference	Document type	Document status
MED		Parts list	Training

Legal owner	Created by	Title, Supplementary title	PR-00.00.000			
KTU	Vinod Raj Begur Venkataraj	Wankel engine				
	Approved by		Rev.	Date	Lang.	Sheet
	Sigitas Kilikevičius		A	2017-05-19	En	1/2

FORMAT	ZONE	NO.	DESIGNATION	NAME	QUANTITY	NOTES
A4		15	PR-00.00.0015	Exhaust manifold	1	
A4		16	PR-00.00.0016	Spark plug	2	
A4		17	PR-00.00.0017	Bush	1	
A4		18	PR-00.00.0018	Front cap seal	1	
A4		19	PR-00.00.0019	Back cap seal	1	
A4		20	PR-00.00.0020	Front cap oil seal	1	
			Standard Items			
				Nut and Bolts		
				ISO 4014 – M12 x 130 S	13	
				ISO 4014 – M6 x 30 S	6	
				ISO 4017 – M6 x 20 S	10	
				AS 1112.3 - C- M12-N	13	
				Bearings		
				IS 1206-A-492239-20	2	
				Washers		
				AS 1237.1 S - 36	13	

Resp. department	Technical reference	Document type	Document status
MED		Parts list	Training

Legal owner	Created by	Title, Supplementary title	PR-00.00.000			
KTU	Vinod Raj Begur Venkataraj	Wankel engine				
	Approved by		Rev.	Date	Lang.	Sheet
	Sigitas Kilikevičius		A	2017-05-18	En	2/2

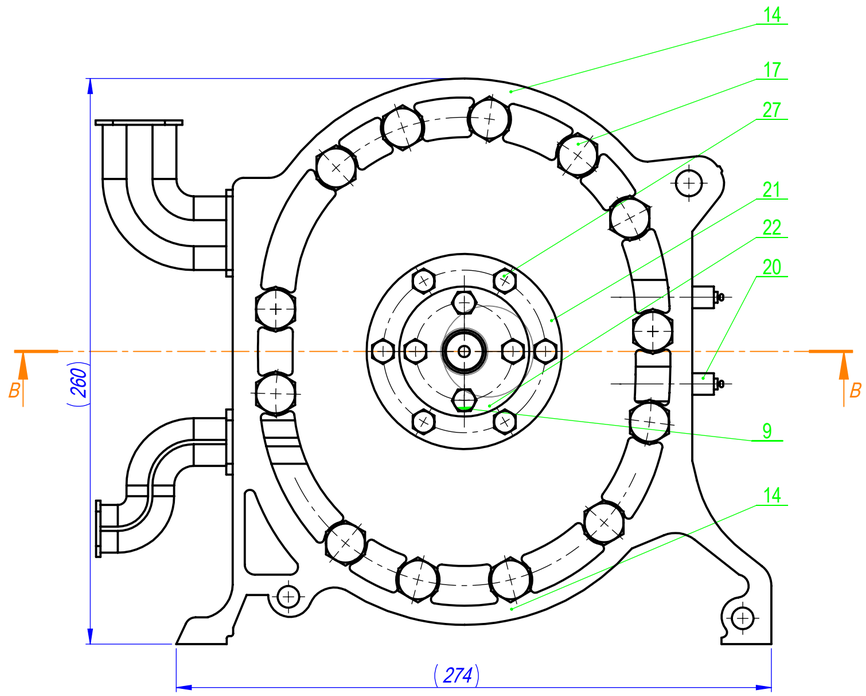

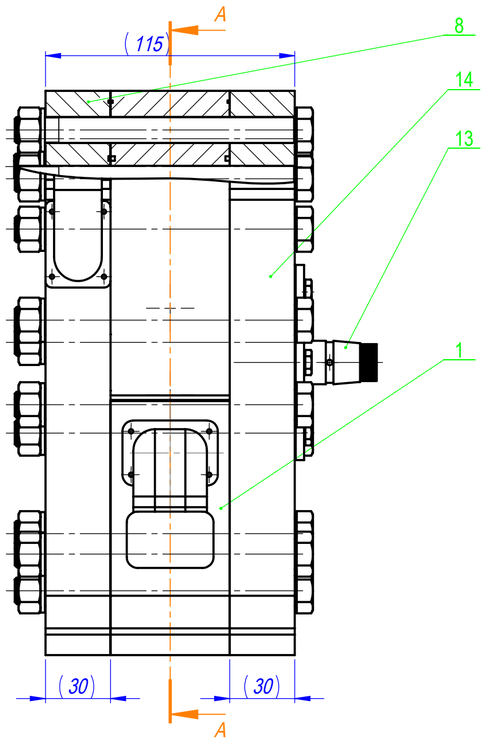

A-A

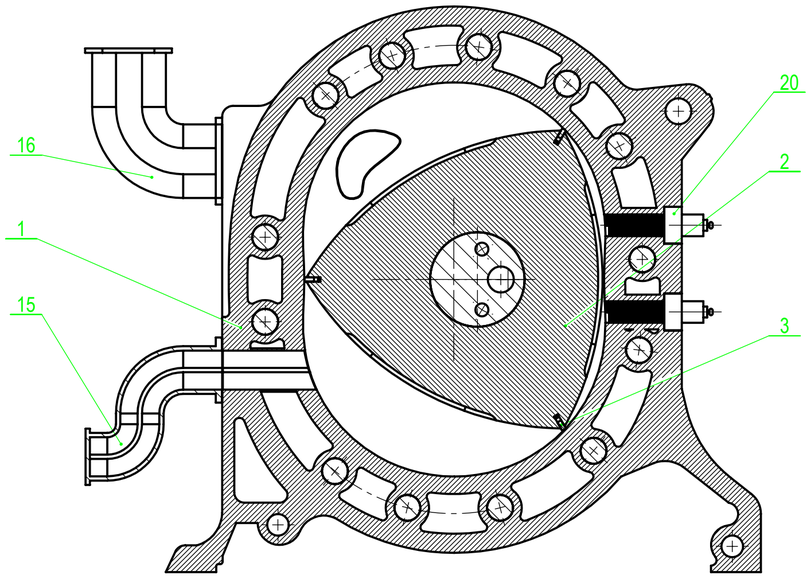

B-B

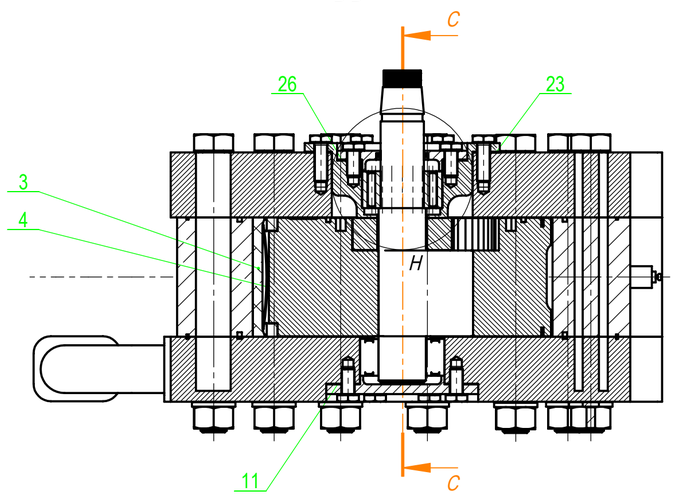

C-C

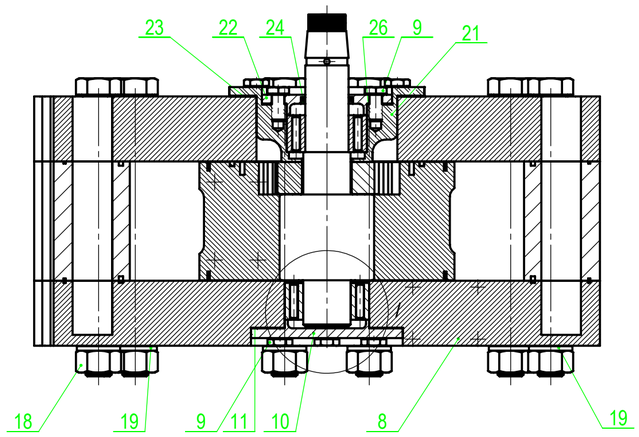

H
1 : 1

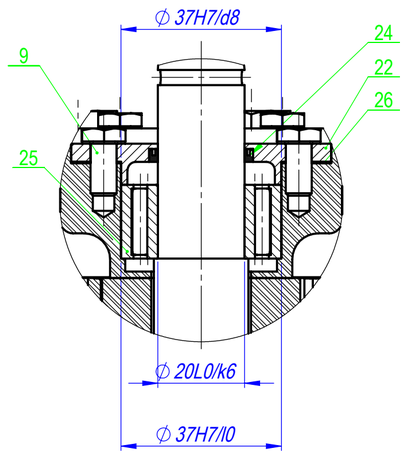

I
1 : 1

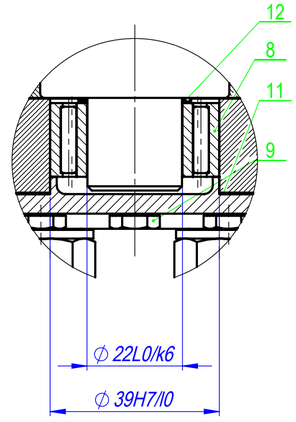

Unspecified tolerance limit according LST EN 22768.

File name	Additional information	Material		Scale 1:2
Resp. department: MED	Technical reference	Document type: Assembly drawing		Document status: Training
Legal owner: KTU	Created by: Vinod Raj Begur Venkataraj	Title, Supplementary title: WANKEL ENGINE	PR-00.00.000 AD	
	Approved by: Sigitas Kilikevičius		Rev.: A / Date: 18/05/2017 / Lang.: En / Sheet: 1/2	

D-D

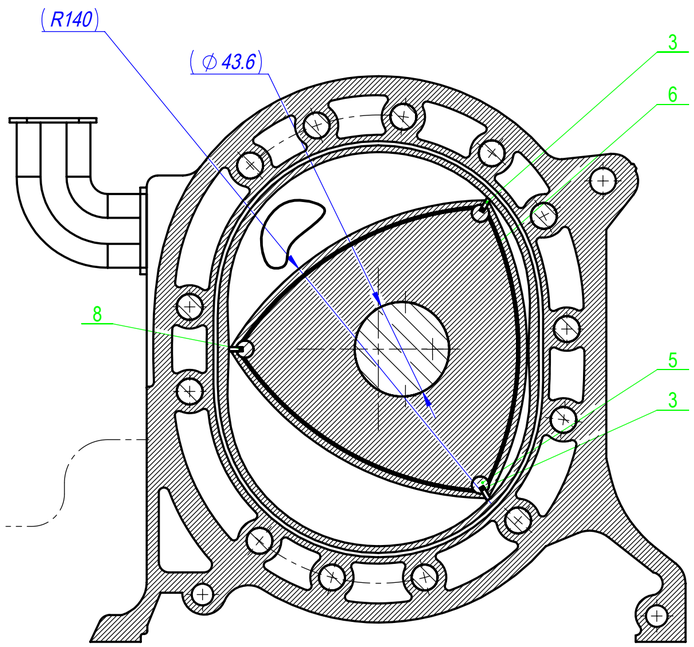

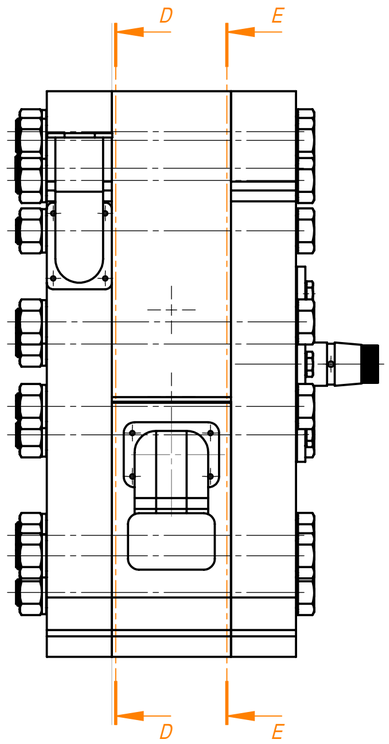

E-E

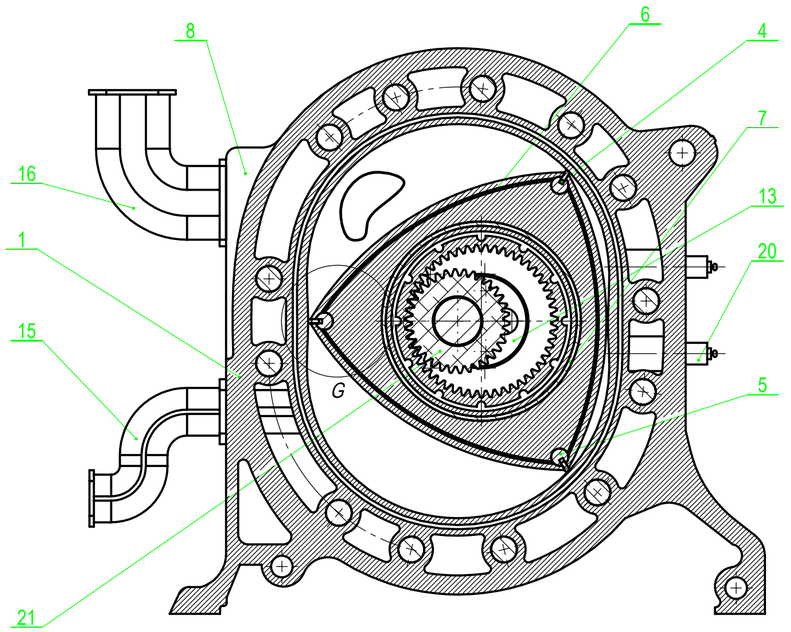

G
2 : 1

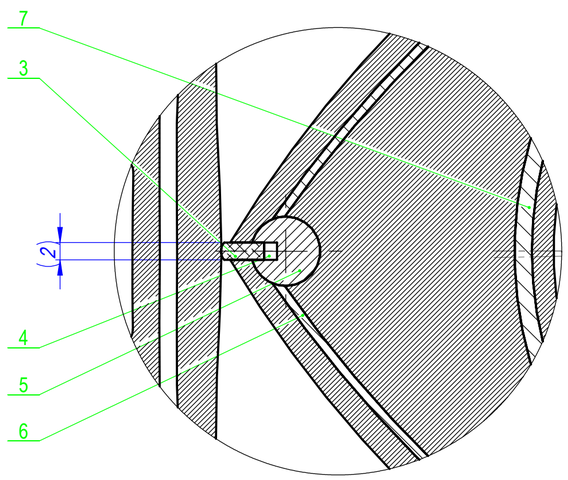

File name	Additional information	Material		Scale 1:2
Resp. department MED	Technical reference	Document type Assembly drawing		Document status Training
Legal owner KTU	Created by Vinod Raj Begur Venkataraj	Title, Supplementary title WANKEL ENGINE	PR-00.00.000 AD	
	Approved by Sigitas Kilikevičius		Rev. A / Date 18/05/2017 / Lang. En / Sheet 2/2	